Adaptive Pseudoinverse Observers for Output Redundant Discrete-Time Linear Systems

Andrea Cristofaro, Luca Zaccarian

Adaptive pseudo-inverse observers for output redundant discrete-time linear systems

Andrea Cristofaro, *Senior Member, IEEE*, and Luca Zaccarian, *Fellow, IEEE*

Abstract

We address the problem of output redundancy in discrete-time linear systems, with the aim of obtaining an optimized combination of sensors for structurally rejecting certain disturbances. We frame our goal as the design problem of a nonlinear observer consisting in a linear Luenberger structure augmented with an adaptive weighted pseudo-inverse combination of the available measurements. A novel optimization algorithm is proposed for the update of the dynamic weights of the pseudo-inverse, together with a selector that overrides the optimizer whenever the pseudo-inverse becomes close to being singular. Numerical simulations on the case study of a discrete-time mechanical system support and validate the proposed architecture.

Index Terms

Linear system observers; Optimization algorithms; Adaptive systems; Output redundancy

I. Introduction and motivation

The presence of redundant inputs and outputs in a control system allows considering secondary objectives, handle critical conditions such as faults or loss of power, and cope with operational or physical constraints. Input redundancy has been widely investigated, to a large extent in the framework of control allocation [1], [2], which is a modular setup where the properties of a redundant set of inputs are exploited in order to formulate a constrained optimization scheme that incorporates both primary and secondary control objectives, see for instance [3]–[8] and the references therein. Fault-tolerant control allocation methods have been proved to be fairly efficient. In particular, having additional degrees of freedom in the control design might be a key advantage in the presence of faults, because the generation of the commanded input can be redistributed on healthy devices [9]–[13].

Differently, output allocation, or *dual redundancy*, is a less explored problem yet interesting and insightful [14]. Methods like the Kalman filter and the extended Kalman filter [15], which aim at the minimization of the covariance error, naturally benefit from the presence of redundant outputs. However such redundancy is typically left unexploited and just implicitly used without a quantitative advantage. On the other hand, alike for the case of actuator redundancy, the clever use of redundant outputs might facilitate the accommodation of sensor faults and or the compensation for biased measurements. In this perspective, some interesting results pertaining safety and reliability of autonomous marine systems have been proposed in [16].

Sensor fault diagnosis is universally recognized as a challenging problem, since no unquestionable methods exist to establish whether a sensor is faulty or not, based on the measured output. Several approaches have been proposed [17], such as robust observers [18], [19], consensus-based schemes [20], adaptive approximation [21]–[23] or statistical methods [24]. Robust observers are typically designed for systems with structured faults by exploiting underlying geometric properties that may lead to a complete fault decoupling, whereas the basic idea of consensus-based approaches is to regard as more trustworthy measurements on which the largest group of sensors agree.

The approach discussed in this paper arises from a somewhat naive observation: among all the possible combinations of a redundant set of outputs, there are certain ones that result to be less sensitive or even insensitive to a given constant bias, or even any time-varying bias preserving the direction in the output space with non-constant amplitude (e.g., due to electromagnetically-induced noise with constant coupling but time-varying amplitude). On the other hand, as the bias signal is typically unknown and hardly predictable, such optimal combinations are likely to be unknown too. In general, when neither faults nor external perturbations are present, an equivalent and full-rank lower dimensional output model can be extracted using a weighted pseudo-inverse, whose weights account for the contribution of each individual sensor. The goal of the paper is to design an adaptation scheme for such weights, with the aim of asymptotically zeroing or, at least, minimizing the resulting effect of the unknown bias in the output estimation error of a given state observer. A similar paradigm has been introduced in

Work supported in part by the INSA-Toulouse via the 2022 visiting professor grant “Mobilités Entrantes”, by the MUR via grant DOCEAT, CUP E63C22000410001, number 2020RTWES4, by the ANR via grant OLYMPIA, number ANR-23-CE48-0006, and by Sapienza University of Rome project DaCARAS, grant n. RP123188E76E8225.

A. Cristofaro is with Department of Computer, Control and Management Engineering, Sapienza University of Rome (Italy), andrea.cristofaro@uniroma1.it

L. Zaccarian is with LAAS-CNRS, Université de Toulouse, CNRS, Toulouse (France) and Dip. di Ingegneria Industriale, University of Trento (Italy), zaccarian@laas.fr

[25], where local results are proposed for continuous-time systems, while a preliminary and partial solution to the discrete-time case has been presented in [26]. As compared to [26], here we provide a new architecture with a new optimizer and a new selector dynamics, for which we can prove asymptotic unbiased estimation and structural rejection. Our architecture is based on the synthesis of two observers, to be used in cascade: the first one is responsible of estimating the bias, while the second one reconstructs the state of the system by performing the output allocation based on a novel line-search optimization algorithm for a quadratic function whose global minimum encodes the best selection of weights in the pseudo-inverse. While our main results are stated for the case of a constant bias, our solution is shown to be readily capable to handle different kinds of output perturbations, such as sensor faults or outliers [27], as shown in our numerical results. It is also worth stressing that a separation principle naturally holds for the proposed observer when used in combination with a feedback controller, allowing to shape separately the closed-loop performances of the feedback control system and of the estimation error.

The paper is organized in seven main sections. In Section II the problem is formally stated, and the design of the asymptotic bias estimator is addressed in Section III. A general architecture for an observer using dynamic output allocation is exploited in Section IV, while a specific minimization algorithm that converges to the optimal weights is formulated in Section V. A description and characterization of the overall observation scheme is reported in Section VI. Finally, in Section VII some numerical examples illustrate the proposed solution and validate the theoretical results, while conclusions are drawn in Section VIII.

Notation. Symbol $\mathbb{R}$ ($\mathbb{R}_{\geq 0}$) denotes the (non-negative) real numbers, and symbol $\mathbb{Z}$ ($\mathbb{Z}_{\geq 0}$) denotes the (non-negative) integer numbers. $\mathbb{R}^p$ denotes the p-dimensional Euclidean space and $\mathbf{e}_i$, $i = 1, ..., p$, denote the vectors of the canonical basis of $\mathbb{R}^p$. The symbol $\mathbb{1}_{n_1 \times n_2}$ indicates the matrix in $\mathbb{R}^{n_1 \times n_2}$ whose entries are all 1, while I_n stands for the identity matrix of dimension n even though the subscript n is often omitted. Given a matrix M, $\mathrm{rk}(M)$ denotes its rank and $\mathrm{Im}(M)$ denotes its image. The n-dimensional unit sphere and the open unit ball are indicated, respectively, with $\mathbb{S}^n$ and $\mathbb{B}^n$ with

$$\mathbb{S}^n := \{\zeta \in \mathbb{R}^{n+1} : |\zeta| = 1\},$$
$$\mathbb{B}^n := \{\zeta \in \mathbb{R}^n : |\zeta| < 1\},$$

so that $\mathbb{S}^{n-1} = \partial\mathbb{B}^n$. Given a vector $v = [v_1 \ \cdots \ v_{n_1}]^T \in \mathbb{R}^{n_1}$ we denote by $\mathrm{diag}(v) \in \mathbb{R}^{n_1 \times n_1}$ the diagonal matrix whose entries are the elements of v. For a discrete time system, we denote $x^+ = f(x)$ as a shortcut notation for $x(k+1) = f(x(k))$, with discrete time $k \in \mathbb{Z}_{\geq 0}$. This shortcut notation allows omitting the explicit dependence on (discrete) time k, except for when it helps the clarity of exposition.

II. Problem definition

Let us consider the linear time-invariant discrete-time plant

$$\begin{aligned} x^+ &= Ax + Bu \\ y &= Cx + \varphi, \end{aligned} \tag{1}$$

where $x \in \mathbb{R}^n$, $u \in \mathbb{R}^m$ and $y \in \mathbb{R}^p$ are state, input and output of the plant, respectively, A, B, C are matrices of appropriate dimensions and $\varphi \in \mathbb{R}^p$ is an unknown but constant bias affecting the output.

For plant (1) we assume that the output y is redundant, in the sense that some measurements are linear combinations of the other ones. We also assume that the state of the plant is detectable from y (otherwise no state estimation could be possible). Finally, we assume that the constant bias/fault φ can be detected from output y, which corresponds to requiring that matrix A can not generate constant responses (namely it has no eigenvalues equal to 1). These assumptions are formalized below.

Assumption 1: Plant (1) is such that the following holds:

1) *Output Redundancy*: the output is redundant, namely there exists an integer q such that $q = \mathrm{rk}(C) < p$.
2) *Detectability of x*: pair (C, A) is detectable;
3) *Detectability of φ*: matrix $A - I$ is nonsingular (namely, matrix A has no eigenvalues equal to 1).

While the first property (redundancy) characterizes the peculiar feature exploited in the scheme proposed in this paper, and is not necessary for estimating x and φ, we emphasize that the two subsequent items in Assumption 1 are indeed necessary to build a finite-time or asymptotic observer of x in the presence of the unknown constant bias φ. In fact, condition 2) is necessary due to standard observability theory for linear systems, while condition 3) is necessary due to linear observability conditions applied to the plant (1) augmented with an exosystem generating a constant output (namely having an eigenvalue equal to 1) and realizing that item 3 is a necessary condition for detectability.

Under item 1 of Assumption 1, there exist matrices $Y \in \mathbb{R}^{p \times q}$, $H \in \mathbb{R}^{q \times n}$ such that

$$q := \mathrm{rk}(C) = \mathrm{rk}(H), \text{ and } C = YH. \tag{2}$$

In particular, since $q < p$, there exists an infinite number of pairs (Y, H) with $C = YH$. For our design, we require the following property on the selection (Y, H).

Assumption 2: Selection (Y, H) satisfies $C = YH$ and the following two properties:

1) *Unitary condition*: the columns of Y are unitary and satisfy $Y^TY = I_q$;

2) *Non-alignment condition*: for each $i = 1, ..., p$, it holds that $\mathbf{e}_i \notin \mathrm{Im}(Y)$.

In the following sections we will develop a line-search optimization algorithm along the coordinate directions $\mathbf{e}_i$, $i = 1, ..., p$. Bearing this in mind, the non-alignment condition is specifically meant to avoid possible saddle-points in the optimization process. In this regard, it is important to stress that Assumption 2 can always be ensured for a suitable selection of Y, under Assumption 1, possibly by recombining the measurements y and redefining matrix C. Indeed, starting from any selection $(Y_\circ, H_\circ)$ such that $Y_\circ$ is full column rank, the following simple procedure can be applied:

- let us define the unitary vector $\mathbf{n} := p^{-\frac{1}{2}} \mathbb{1}_{p\times 1}$ and observe that the space $\mathbf{n}^\perp$ contains none of the coordinate axis by construction;
- pick an orthogonal transformation[1] Σ mapping any given unitary vector of $Y^\perp$ into $\mathbf{n}$;
- define $H = (Y_\circ^T Y_\circ)^{\frac{1}{2}} H_\circ$ and $Y = \Sigma Y_\circ (Y_\circ^T Y_\circ)^{-\frac{1}{2}}$.

With such a modified selection of H and Y it is immediate to see that Assumption 2 holds for a modified output matrix $C_{\text{mod}} = \Sigma C$. Note also that detectability of (C, A) coincides with detectability of (C_{mod}, A) because Σ is square and full rank.

Example 1: To better illustrate the previous output transformation procedure, let us consider the output matrix

$$C = \begin{bmatrix} 1 & 0 & 0 & 0 \\ 0 & 1 & 0 & 0 \\ 1 & -1 & 0 & 0 \end{bmatrix} \tag{3}$$

An intuitive decomposition for the output matrix is given by the selection $(Y_\circ, H_\circ)$ with

$$Y_\circ = \begin{bmatrix} 1 & 0 \\ 0 & 1 \\ 1 & -1 \end{bmatrix}, \quad H_\circ = \begin{bmatrix} 1 & 0 & 0 & 0 \\ 0 & 1 & 0 & 0 \end{bmatrix}$$

where $H_\circ$ essentially keeps the two independent output channels decoupled. Such a simple selection does not meet the unitary condition, but performing the transformation

$$Y = Y_\circ (Y_\circ^T Y_\circ)^{-\frac{1}{2}} = \begin{bmatrix} \frac{3+\sqrt{3}}{6} & \frac{3-\sqrt{3}}{6} & \frac{1}{\sqrt{3}} \\ \frac{3-\sqrt{3}}{6} & \frac{3+\sqrt{3}}{6} & -\frac{1}{\sqrt{3}} \end{bmatrix}^T \tag{4a}$$

$$H = (Y_\circ^T Y_\circ)^{\frac{1}{2}} H_\circ = \begin{bmatrix} \frac{3+\sqrt{3}}{2\sqrt{3}} & \frac{-3+\sqrt{3}}{2\sqrt{3}} & 0 \\ \frac{-3+\sqrt{3}}{2\sqrt{3}} & \frac{3+\sqrt{3}}{2\sqrt{3}} & 0 \end{bmatrix} \tag{4b}$$

we are guaranteed to deal with a selection (Y, H) where the matrix Y satisfies Assumption 2.

For any selection of H satisfying (2), since we assume detectability in item 2 of Assumption 1, then pair (H, A) is also detectable and, in the absence of the bias φ, a full order Luenberger observer can be designed:

$$\hat{x}^+ = A\hat{x} + Bu + L(Hx - H\hat{x}) \tag{5}$$

where Hx can be obtained from $y = Cx$ by pre-multiplication with any pseudo-inverse of Y and where L is a suitable output error injection gain ensuring that any solution satisfies $|x_k - \hat{x}_k| \to 0$ as k tends to $+\infty$.

The scope of this paper is to develop a design procedure for an unbiased observer, i.e. an observer that, using the injection of the redundant output y, guarantees the same performance as the nominal observer (5), despite the presence of the fault/bias φ.

III. Asymptotic bias estimation

As a first ingredient of our scheme, we exploit Assumption 1 to design an asymptotic estimate $\hat{\varphi}$ of the bias φ. To this end, we first observe that φ always admits a decomposition of the following form:

$$\varphi = Y w_\varphi + \varphi_o, \tag{6}$$

with $w_\varphi \in \mathbb{R}^p$ and where $\varphi_o \in [\mathrm{Im}(Y)]^\perp$ satisfies $Y^T \varphi_o = 0$. Vector φ_o can be readily extracted from the output by projecting measurement y onto $[\mathrm{Im}(Y)]^\perp$ at any time $k \in \mathbb{Z}_{\geq 0}$, as follows:

$$\varphi_o = (I - Y\mathbb{P}_Y)y, \quad \mathbb{P}_Y := (Y^T Y)^{-1} Y^T,$$

where $\mathbb{P}_Y$ can be well seen as projection-like matrix. Thanks to item 2 of Assumption 1, we can select a Luenberger gain M such that $A - MH$ is a Schur matrix (namely its eigenvalues have magnitude smaller than one). Using this output injection gain, we introduce an observer with the scope of estimating w_φ:

$$\xi^+ = A\xi + Bu + M\mathbb{P}_Y(y - C\xi). \tag{7a}$$

[1] A simple algorithm can be designed by operating on the singular value decomposition of Y.

The asymptotic estimate $\hat{\varphi}$ of φ can be then determined as follows:

$$\eta := \mathbb{P}_Y y - H\xi \tag{7b}$$
$$\hat{\varphi} := Y(I + H(I-A)^{-1}M)\eta + (I - Y\mathbb{P}_Y)y, \tag{7c}$$

where the output gain in (7c) is well defined due to item 3 of Assumption 1. The effectiveness of (7) at estimating φ is established in the next proposition.

Proposition 1: Under Assumption 1, if matrix $A - MH$ is Schur, then the difference $\hat{\varphi} - \varphi$ converges exponentially to zero for (7).

Proof: Let us introduce the estimation error $\varepsilon := x - \xi$. The error dynamics reads as:

$$\varepsilon^+ = (\underbrace{A - MH}_{:=A_{cl}})\varepsilon - Mw_\varphi. \tag{8}$$

Based on the variation of constants formula (see, e.g., [28, page 51]), and keeping in mind that $A_{cl} := A - MH$ being Schur implies that $\sum_{i=0}^{k} A_{cl}^i$ converges exponentially (as k tends to ∞) to $(I - A_{cl})^{-1}$, we obtain the following form for the explicit solution to (8):

$$\begin{aligned}\varepsilon_k &= A_{cl}^k\varepsilon_0 - \sum_{i=0}^{k-1} A_{cl}^i M w_\varphi \\ &= A_{cl}^k\varepsilon_0 + \left(\sum_{i=0}^{\infty} A_{cl}^i - \sum_{i=0}^{k-1} A_{cl}^i\right) M w_\varphi - (I - A_{cl})^{-1} M w_\varphi \\ &= -(I - A_{cl})^{-1} M w_\varphi + \delta_k,\end{aligned} \tag{9}$$

where $\delta_k := A_{cl}^k\varepsilon_0 + \left(\sum_{i=0}^{\infty} A_{cl}^i - \sum_{i=0}^{k-1} A_{cl}^i\right) M w_\varphi$ converges exponentially to zero because A_{cl} is Schur.

Let us also observe that, using $C = YH$ and (6), output η in (7b) can be expressed as a function of ε as follows:

$$\begin{aligned}\eta &= (Y^TY)^{-1}Y^T(\underbrace{YHx + \varphi}_{y}) - H\xi \\ &= H\varepsilon + (Y^TY)^{-1}Y^T(Yw_\varphi + \varphi_o) = H\varepsilon + w_\varphi,\end{aligned} \tag{10}$$

where we used $Y^T\varphi_o = 0$. The identity above can be combined with (9) to obtain

$$\eta = (I - H(I - A_{cl})^{-1}M)w_\varphi + H\delta := C_\eta w_\varphi + H\delta, \tag{11}$$

where matrix C_η can be suitably partitioned, using Woodbury's matrix inversion lemma, and using invertibility of $I - A$ (from item 3 of Assumption 1) to obtain:

$$C_\eta = I - H(I - A + MH)^{-1}M = (I + H(I-A)^{-1}M)^{-1} \tag{12}$$

Combining this identity with the output equation (7c) and expression (10), we get:

$$\begin{aligned}\hat{\varphi} &= YC_\eta^{-1}(C_\eta w_\varphi + H\delta) + (I - Y\mathbb{P}_Y)y \\ &= YC_\eta^{-1}H\delta + Yw_\varphi + \varphi_o = YC_\eta^{-1}H\delta + \varphi,\end{aligned}$$

where we used (6) and where the sequence $k \mapsto \delta_k$ converges exponentially to zero, thus completing the proof. ■

Remark 1: Under the stronger requirement of full observability of the pair (A, H) the bias estimator may also be made deadbeat, with $\sigma(A - MH) = \{0\}$. This could be a desirable feature to accelerate the convergence but, as a drawback, the accuracy might deteriorate when the measurements are noisy. As a general rule of thumb, supported by the good performances obtained in our simulation tests, it might be preferable to shape the bias estimator with a faster dynamics than the one of the state observer. In this respect, one needs to bear in mind that, in order to avoid peaks during the transient when a fast observer is used, it might also be wise to enhance the design with an anti-peaking mechanism (see for example [29], [30]). ○

IV. An observer using adaptive pseudoinverses

In this section we investigate the design of enhanced observers by using the estimate $\hat{\varphi}$ of bias φ given by (7) and simultaneously exploiting the sensor redundancy with the aim of reducing the effect of noisy measurements and bias variations on the estimation performance.

The proposed scheme, represented in Figure 1 corresponds to the cascade interconnection of the asymptotic bias estimator presented in Section III and a nonlinear estimator based on a parametric pseudoinverse. This second estimator is based on the cascaded interconnection between an optimizer, having state $z \in \mathbb{R}^p$, followed by a selector, having state $s \in \mathbb{R}^p$, and finally the observer dynamics, whose state $\hat{x}$ is the unbiased estimate of the plant state x.

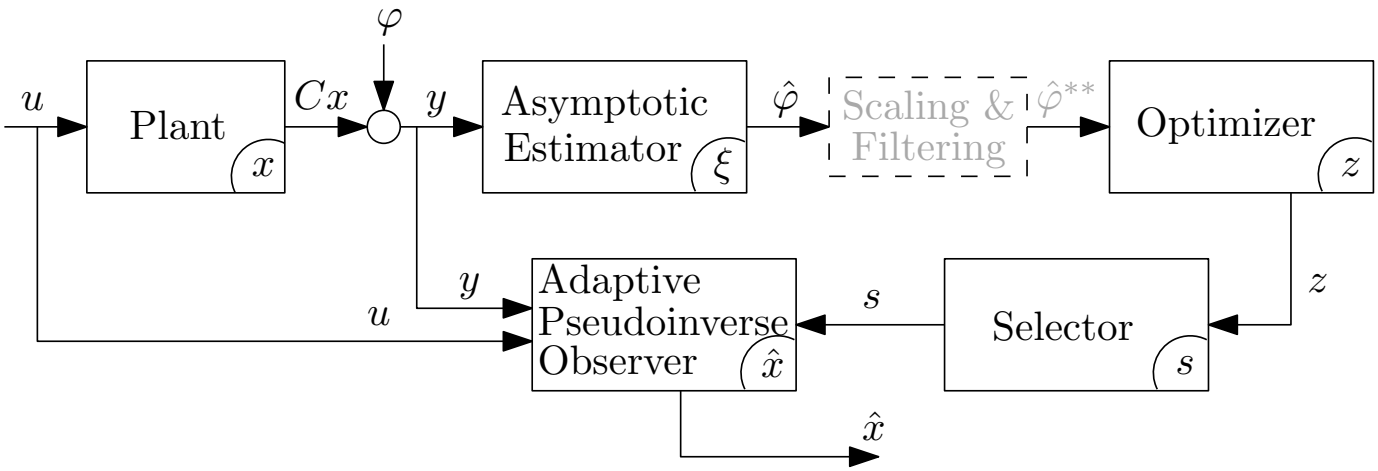

Fig. 1. Block diagram of the proposed estimation scheme based on parametric pseudoinverses.

A. Observer architecture and error system

Similar to (5), given any gain matrix L such that $A - LH$ is Schur, we construct the following asymptotic observer:

$$\begin{aligned} \hat{x}^+ &= A\hat{x} + Bu + L\Pi(s)(y - \hat{y}) \\ \hat{y} &= C\hat{x}. \end{aligned} \tag{13}$$

The additional state $s \in \mathbb{R}^p$, whose dynamics is specified below, is selected to perform an on-line adaptation of matrix function Π, which corresponds to the weighted pseudoinverse

$$\Pi(s) := R(s)^{-1}\Gamma(s) := (\underbrace{Y^T \operatorname{diag}(s) Y}_{=:R(s)})^{-1} \underbrace{Y^T \operatorname{diag}(s)}_{=:\Gamma(s)}. \tag{14}$$

The goal in the selection of s is to ensure that it automatically extracts the "best" information content among the redundant measurements y through $\Pi(s)$. To this end, we first observe that $\Pi(s)$ is scale invariant, i.e. $\Pi(s) = \Pi(\mu s)$ for any scalar $\mu \neq 0$, and for this reason it is helpful to restrict the vector s to lie on the unit sphere $\mathbb{S}^{p-1}$. Moreover, we observe that map Π in (14) is only well defined if matrix R is invertible. As a consequence, we choose s as the output of a so-called "selector" dynamics (see Figure 1) whose state s is constrained to only evolve in the following set:

$$\mathcal{S}_\epsilon := \{s \in \mathbb{S}^{p-1} : \ |\det(R(s))| \geq \epsilon\}, \tag{15}$$

which is compact because it is the intersection between the compact set $\mathbb{S}^{p-1}$ and a closed unbounded set.

To complete our observation scheme, we embed in the system a further dynamical system, the "optimizer" in Figure 1, whose state $z \in \mathbb{S}^{p-1}$ is the result of an online optimization aimed at providing a desirable candidate for the parameter s of the weighted pseudoinverse, as long as it belongs to the set $\mathcal{S}_\epsilon$ where s is allowed to evolve.

More specifically, the dynamics of the optimizer and the selector blocks in Figure 1 are chosen as the following inclusions

$$z^+ \in G_z(z, \hat{\varphi}), \tag{16}$$

$$s^+ \in G_s(s, z) := \begin{cases} z & \text{if } z \notin \overline{\mathbb{S}^{p-1} \setminus \mathcal{S}_\epsilon}, \\ s & \text{if } z \notin \mathcal{S}_\epsilon, \\ \{s, z\} & \text{otherwise.} \end{cases} \tag{17}$$

Let us first comment on the selector dynamics G_s in (17), which selects the optimizer output z whenever z belongs to the interior of $\mathcal{S}_\epsilon$ relative to $\mathbb{S}^{p-1}$ (the notation in the first case of (17) essentially excludes the boundary of the set in (15) relative to $\mathbb{S}^{p-1}$). When z is not in the allowable set $\mathcal{S}_\epsilon$ for s, then the state s remains unchanged across the jump. Finally, the third case in (17) ensures that G_s is outer semicontinuous because it allows for both selections of s and z at the boundary. Outer semicontinuity is desirable because it induces well-posedness of the dynamics, thus enabling us to exploit reduction theorems [31] in our proofs.

Let us now focus on the optimizer, whose goal is to converge to a value of $z \in \mathbb{S}^{p-1}$ that is in the kernel of $\Gamma(\varphi)$, as clarified below. First, we observe that for any pair $v_1, v_2 \in \mathbb{R}^p$ the following identity holds $\operatorname{diag}(v_1)v_2 = \operatorname{diag}(v_2)v_1$, and therefore

$$\Gamma(s)\varphi = \Gamma(\varphi)s, \tag{18}$$

where Γ has been defined in (14).

By developing the output injection term in (13), we may then appreciate the importance of the product $\Gamma(s)\varphi$. Indeed, we get, also using (18),

$$\begin{aligned} L\Pi(s)(y-\hat{y}) &= LR(s)^{-1}\Gamma(s)(YHx+\varphi-YH\hat{x}) \\ &= LR(s)^{-1}\Gamma(s)YH(x-\hat{x}) + LR(s)^{-1}\Gamma(s)\varphi \\ &= L(Hx-H\hat{x}) + LR(s)^{-1}\Gamma(\varphi)s, \end{aligned} \tag{19}$$

where we used $R(s)^{-1}\Gamma(s)Y = R(s)^{-1}Y^T\,\mathrm{diag}(s)Y = I$.

Combining equation (19) with observer (13) and plant (1), we can introduce the error dynamics of the pseudoinverse observer, whose states comprise the estimation error $e := x - \hat{x}$, and the optimizer and selector states $z \in \mathbb{S}^{p-1}$ and $s \in \mathcal{S}_\epsilon$, and reads

$$\begin{aligned} e^+ &= (A-LH)e + LR(s)^{-1}\Gamma(\varphi)s, \\ s^+ &\in G_s(s,z), \qquad\qquad (e,s,z) \in \mathcal{E}, \\ z^+ &\in G_z(z,\hat{\varphi}), \end{aligned} \tag{20}$$

with $\mathcal{E} := \mathbb{R}^n \times \mathcal{S}_\epsilon \times \mathbb{S}^{p-1}$ being the (forward invariant) set where the state (e,s,z) is allowed to evolve, and with the input $\hat{\varphi} \in \mathbb{R}^p$ coming from observer (7).

B. Stability of the error dynamics

The error dynamics (20) illustrates the effectiveness of the proposed solution in terms of providing an observer that, in the presence of the unknown bias φ, structurally recovers the estimation error transient experienced with the unbiased dynamics (5). Such a recovery is however only possible if the fault effect $R(s)^{-1}\Gamma(\varphi)s$ becomes zero, at least asymptotically. This is achieved here by ensuring *two goals:* on the one hand that the optimizer converges to an asymptotic value $z^\star$ satisfying $\Gamma(\varphi)z^\star = 0$, and on the other hand that such an optimal $z^\star$ is asymptotically assumed by s, through the selector dynamics (17).

The *first goal* of asymptotically obtaining $\Gamma(\varphi)z = 0$ motivates defining the following subset of $\mathbb{S}^{p-1}$

$$\mathcal{Z}^\star := \{z \in \mathbb{S}^{p-1} : \Gamma(\varphi)z = 0\}, \tag{21}$$

and introducing a useful property of the set-valued function G_z in (16). This property will be guaranteed, under Assumptions 1 and 2 by the construction proposed later in Section V.

Property 1: The set-valued map G_z in (16) is nonempty, locally bounded and outer semi-continuous relative to $\mathbb{S}^{p-1} \times \mathbb{R}^p$. Moreover, the following decrease condition holds:

$$z^+ \in G_z(z,\varphi) \;\Rightarrow\; (\Gamma(\varphi)z^+ = 0) \text{ or } (|\Gamma(\varphi)z^+| < |\Gamma(\varphi)z|). \tag{22}$$

Property 1 ensures that, as long as G is fed with the correct bias signal φ, it produces a set of possible selections for the next value of z, that leads to an improvement of the filtering action in (19), unless its value is already zero. This corresponds to ensuring a decreasing distance to the set $\mathcal{Z}^\star$ in (21).

Let us now discuss the *second goal* that, asymptotically, the value $z^\star$ provided by the optimizer is actually assumed by the selector state s through dynamics (17). To this end, it is enough to assume that the closed complement of (15), relative to $\mathbb{S}^{p-1}$ is disjoint from the desirable set $\mathcal{Z}^\star$, asymptotically approached by z. This is clarified in the next property, whose validity is studied in various cases characterized in Section VI.

Property 2: The two closed sets $\mathcal{Z}^\star$ and $\overline{\mathbb{S}^{p-1} \setminus \mathcal{S}_\epsilon}$ (both subsets of $\mathbb{S}^{p-1}$) are disjoint.

Since the second set considered in Property 2 coincides with the set mentioned at the first item of the dynamics in (17), then Property 2 ensures that for any $z \in \mathcal{Z}^\star$, the inclusion in (17) selects z rather than s for the next value s^+.

Based on Properties 1 and 2, we can now state the following result, which is a second important baseline result for the proposed scheme. Its proof is reported in Section IV-C.

Proposition 2: If Properties 1 and 2 hold, then for any L ensuring that $A - LH$ is Schur, the compact set:

$$\begin{aligned} \mathcal{A}_e := \{(e,s,z) \in \mathbb{R}^n \times \mathcal{S}_\epsilon \times \mathbb{S}^{p-1} : \\ z \in \mathcal{Z}^\star, \Gamma(\varphi)s = 0, e = 0\} \end{aligned} \tag{23}$$

is globally asymptotically stable for the error dynamics (20) driven by $\hat{\varphi}_k = \varphi$ for all k.

Note that dynamics (20) becomes an autonomous system when $\hat{\varphi}_k = \varphi$, so that asymptotic stability of $\mathcal{A}_e$ is in the classical sense.

Our main theorem below follows from Propositions 1 and 2. Before its statement, let us revisit the error dynamics (8) and notice that, whenever $A - MH$ is Schur, ε converges exponentially to the unique equilibrium:

$$\varepsilon^\star := -(I - (A - MH))^{-1}Mw_\varphi. \tag{24}$$

Then, following Proposition 1 and using (10), we also obtain that $\varepsilon = \varepsilon^\star$ implies:

$$\begin{aligned}\hat{\varphi} &= Y(I + H(I-A)^{-1}M)(\mathbb{P}_Y y_k - H\xi_k) + \varphi_o \\ &= YC_\eta^{-1}(w_\varphi + H\varepsilon^\star) + \varphi_o \\ &= YC_\eta^{-1}(w_\varphi - H(I - A + MH)^{-1}Mw_\varphi) + \varphi_o \\ &= YC_\eta^{-1}C_\eta w_\varphi + \varphi_o = Yw_\varphi + \varphi_o = \varphi,\end{aligned}$$

where we adopted the notation in (12).

Based on the above derivations, our goal is to focus on the following compact set:

$$\begin{aligned}\mathcal{A} := \{(\varepsilon, e, s, z) \in \mathbb{R}^n \times \mathbb{R}^n \times \mathcal{S}_\epsilon \times \mathbb{S}^{p-1} : \\ s = z, \Gamma(\varphi)z = 0, \varepsilon = \varepsilon^\star, e = 0\}\end{aligned} \tag{25}$$

whose desirable stability properties are established in the main result below, proven in the next section.

Theorem 1: Under Assumption 1, consider any pair of gains M and L such that $A - LH$ and $A - MH$ are Schur. If Properties 1 and 2 hold, then the compact set $\mathcal{A}$ in (25) is globally asymptotically stable for the ensuing error dynamics (8), (20).

C. Proofs of Proposition 2 and Theorem 1

The proofs exploit the intrinsic cascaded structure of the proposed observers. In particular, we will use the following corollary of [31, Cor. 4.8].

Lemma 1: Consider a constrained nonlinear difference inclusion

$$\xi^+ \in \bar{G}(\xi), \quad \xi \in \mathcal{D}, \tag{26}$$

where $\mathcal{D}$ is a closed subset of $\mathbb{R}^s$, and $\bar{G} : \mathbb{R}^s \rightrightarrows \mathbb{R}^s$ is outer semi-continuous, locally bounded and non-empty relative to $\mathcal{D}$. Assume that

1) a closed set $\mathcal{M} \subset \mathbb{R}^s$ is stable and globally attractive (therefore strongly forward invariant) for (26);
2) the compact set $\mathcal{M}_\circ \subset \mathcal{M}$ is stable and globally attractive for (26) relative to $\mathcal{M}$ (namely, for the restricted dynamics $\xi^+ \in \bar{G}(\xi),\ \xi \in \mathcal{M}$).

Then the set $\mathcal{M}_\circ$ is asymptotically stable for (26), with basin of attraction coinciding with the largest set of initial conditions from which all solutions are bounded. In particular, if all solutions are bounded, then the set $\mathcal{M}_\circ$ is globally asymptotically stable for (26).

Based on Lemma 1 we may now prove Proposition 2.

Proof of Proposition 2. Let us first apply Lemma 1 to dynamics (20) with the following selections of $\mathcal{D}$ and $\mathcal{M}$

$$\begin{aligned}\mathcal{D}_1 &= \{(e, s, z) : e \in \mathbb{R}^{2n}, s \in \mathcal{S}_\epsilon, z \in \mathcal{Z}^\star\}, \\ \mathcal{M}_1 &= \{(e, s, z) : e \in \mathbb{R}^{2n}, s, z \in \mathcal{Z}^\star \cap \mathcal{S}_\epsilon\},\ \mathcal{M}_\circ = \mathcal{A}_e,\end{aligned} \tag{27}$$

where $\mathcal{A}_e$ has been introduced in (23). Let us prove the two items of Lemma 1 for selection (27). *Item 1*: first notice that due to Property 2, we have

$$\mathcal{Z}^\star = \mathcal{Z}^\star \cap \mathcal{S}_\epsilon. \tag{28}$$

Due to Property 2, $z \in \mathcal{Z}^\star$ implies $z^+ \in \mathcal{Z}^\star$, namely $\mathcal{Z}^\star$ is forward invariant for the dynamics of z. Moreover, due to (28), G_s always returns z, so that $s \in \mathcal{Z}^\star$ after one time step, thus proving item 1 of Lemma 1. *Item 2*: Since in $\mathcal{M}_1$ we have $\Gamma(\varphi)s = 0$, then the dynamics of e in (20) is unperturbed and linear, and the assumption that $A - LH$ be Schur implies item 2 of Lemma 1. Boundedness of solutions finally follows from the fact that z and s are bounded because they evolve in (subsets of) the bounded set $\mathbb{S}^{p-1}$, and the dynamics of e is linear exponentially stable affected by a bounded perturbation. Indeed, the forcing term $LR(s)^{-1}\Gamma(\varphi)s$ is bounded from boundedness of s and from the fact that the determinant of R is lower bounded by ϵ in the set $\mathcal{S}_\epsilon$, which results in uniform boundedness of $R(s)^{-1}$. Finally, standard discrete-time BIBO stability properties of the linear dynamics implies boundedness of e. Since all the properties of Lemma 1 hold, then set $\mathcal{M}_\circ$ is globally asymptotically stable for the dynamics (20) restricted to $\mathcal{D}_1$ in (27).

As a second step, let us now apply Lemma 1 to dynamics (20) with the following selections of $\mathcal{D}$ and $\mathcal{M}$

$$\begin{aligned}\mathcal{D}_2 &= \{(e, s, z) : e \in \mathbb{R}^{2n}, s \in \mathcal{S}_\epsilon, z \in \mathbb{S}^{p-1}\}, \\ \mathcal{M}_2 &= \mathcal{D}_1,\ \mathcal{M}_\circ = \mathcal{A}_e,\end{aligned} \tag{29}$$

with $\mathcal{D}_1$ as in (27) and $\mathcal{A}_e$ as in (23) (notice that $\mathcal{M}_\circ$ is unchanged). For the selections in (29), we prove the two items of Lemma 1. Since $\mathcal{M}_2 = \mathcal{D}_1$ and $\mathcal{M}_\circ$ is the same as in (27), then item 2 correspondds to proving GAS of $\mathcal{M}_\circ$ for the dynamics restricted to $\mathcal{D}_1 = \mathcal{M}_2$ and it has been shown in the first part of this proof (by the first application of Lemma 1).

For proving item 1 of Lemma 1, consider the Lyapunov-like function $|\Gamma(\varphi)z|^2$, which is positive definite with respect to $\mathcal{Z}^\star$ in (21) relative to the compact set $\mathbb{S}^{p-1}$. From compactness of $\mathcal{Z}^\star$ and $\mathbb{S}^{p-1}$, Property 1 clearly implies a uniform decrease of this Lyapunov function and then the discrete-time Lyapunov theorem implies global asymptotic stability of $\mathcal{Z}^\star$ for dynamics $z^+ \in G_z(z,\varphi)$, thus proving item 1 of Lemma 1. Finally, boundedness of solutions is proven by following the same steps as the previous iteration of Lemma 1.

The global asymptotic stability result established by this second iteration of Lemma 1 coincides with the statement of the proposition, thus completing the proof. ■

Proof of Theorem 1 The proof follows very similar arguments to those of the previous proof by performing a third iteration of Lemma 1.

In particular, we first notice that from the properties established in Proposition 1, the vector $\varepsilon^\star$ introduced in (24) is such that the ensuing coordinate shift $\tilde{\varepsilon} := \varepsilon - \varepsilon^\star$ obeys dynamics:

$$\begin{aligned} \tilde{\varepsilon}^+ &= (A - MH)\tilde{\varepsilon} \\ \tilde{\varphi} &:= \hat{\varphi} - \varphi = YC_\eta^{-1}\tilde{\varepsilon} := \tilde{C}\tilde{\varepsilon}. \end{aligned} \tag{30}$$

As a result, we may prove the theorem by focusing on the dynamics arising from combining (30) with the remaining dynamics arising from (20):

$$\begin{aligned} e^+ &= (A - LH)e + LR(s)^{-1}\Gamma(\varphi)s, \\ s^+ &\in G_s(s,z) \\ z^+ &\in G_z(z, \varphi + \tilde{C}\tilde{\varepsilon}). \end{aligned} \tag{31}$$

To this end, the attractor $\mathcal{A}$ in (25) can be expressed as

$$\begin{aligned} \mathcal{A} := \{(\tilde{\varepsilon}, e, s, z) \in \mathbb{R}^{2n} \times \mathcal{S}_\epsilon \times \mathbb{S}^{p-1} : \\ s, z \in \mathcal{Z}^\star \cap \mathcal{S}_\epsilon, e = 0, \tilde{\varepsilon} = 0\}, \end{aligned}$$

with the compact set $\mathcal{Z}^\star$ and $\mathcal{S}_\epsilon$ defined in (21) and (15), respectively.

To prove GAS of $\mathcal{A}$ we apply again Lemma 1, with the selections $\mathcal{M}_\circ = \mathcal{A}$ and

$$\begin{aligned} \mathcal{D}_3 &= \mathbb{R}^n \times \mathbb{R}^n \times \mathcal{S}_\epsilon \times \mathbb{S}^{p-1} \\ \mathcal{M}_3 &= \{(\tilde{\varepsilon}, e, s, z) : \ s \in \mathcal{S}_\epsilon, z \in \mathbb{S}^{p-1}, e \in \mathbb{R}^n, \tilde{\varepsilon} = 0\}, \end{aligned} \tag{32}$$

where we see that $\mathcal{M}_3 = \{0\} \times \mathcal{D}_2$, while $\mathcal{D}_3$ is the set of all allowable values of the error variables.

With this third selection in (32) item 1 of Lemma 1 follows from linearity of the error dynamics in (30), while item 2 follows from Proposition 2. Finally, the fact that all solutions are bounded can be proven following identical steps to those of the proof of Proposition 2. ■

D. Robustness, scale invariance and low-pass filtering

In a practical scenario, it is unreasonable to assume that the observation scheme of Figure 1 only operates in the nominal conditions considered in Theorem 1. In fact, potential fragility of nonlinear observation schemes has been long known as a problematic issue, a matter well characterized in [32, §5], where input-to-state stability (ISS) properties of the error dynamics is emphasized as being a desirable property. Exploiting the intrinsic robustness of well-posed dynamical systems established in [33, Ch 7], we prove here ISS properties of the error dynamics (8), (20) when including a generic perturbation $d = (d_x, d_y)$ in the plant dynamics (1) as follows

$$x^+ = Ax + Bu + d_x, \quad y = Cx + \varphi + d_y, \tag{33}$$

thus establishing robustness of the result of Theorem 1.

Theorem 2: Under Assumption 1, consider any pair of gains M and L such that $A - LH$ and $A - MH$ are Schur. If Properties 1 and 2 hold, then there exists a class $\mathcal{KL}$ function $\beta_\circ$ and a class $\mathcal{K}$ function $\gamma_\circ$ such that the solutions $\xi = (\varepsilon, e, s, z)$ of the error dynamics (8), (20) resulting from a perturbed plant, as in (33), enjoy the ISS bound

$$|\xi(j)|_{\mathcal{A}} \leq \beta_\circ(|\xi(0)|_{\mathcal{A}}) + \gamma(\|d\|_\infty), \tag{34}$$

with the compact set $\mathcal{A}$ as in (25), and where $\|d\|_\infty = \sup_{j\geq 0} |d(j)|$.

Proof: Due to linearity of the error dynamics characterized in (30) for the linear observer (7), exponential stability implies finite-gain ISS from the perturbation d to the estimation error $\tilde{\varepsilon}$ and the output error $\tilde{\varphi} = \hat{\varphi} - \varphi$. Let us now study the effect of these nonzero errors $\tilde{\varepsilon}, \tilde{\varphi}$ on the remaining difference inclusion (31), where we recall that the corresponding state (e, s, z) evolves in the set $\mathbb{R}^n \times \mathcal{S}_\epsilon \times \mathbb{S}^{p-1}$. Since the set $\mathcal{A}$ is compact, and the right-hand side of (31) is well posed in the sense of [33, As. 6.5] (it is nonempty, outer semi-continuous and locally bounded), then the global asymptotic stability established in Theorem 1 implies semiglobal practical asymptotic stability, as per [33, Lemma 7.20]. Considering dynamics (31), since

s and z are bounded (they evolve in the bounded set $\mathcal{S}_\epsilon \times \mathbb{S}^{p-1}$) and since $A - LH$ is Schur and the perturbation term $LR(s)^{-1}\Gamma(\varphi)s$ is bounded, then semiglobal practical asymptotic stability implies global practical asymptotic stability. Global practical asymptotic stability corresponds to a specific notion of small-signal ISS of $\mathcal{A}$, namely there exist functions $\beta_\circ \in \mathcal{KL}$ and $\gamma_\circ \in \mathcal{K}$ and a (typically small) $\overline{d} > 0$ such that for any signal d satisfying $\|d\|_\infty \leq \overline{d}$, the ISS bound (34) holds.

Let us now focus on a global extension of the bound. For each selection of d such that $\|d\|_\infty > \overline{d}$, both the substates $\tilde{\varepsilon}$ and e in the error dynamics (30) and (31) remain bounded because $A - LH$ and $A - MH$ are Schur, and the perturbation term $LR(s)^{-1}\Gamma(\varphi)s$ is bounded too. Moreover, the remaining states s and z are bounded by definition. This implies that functions $\beta_\circ$ and $\gamma_\circ$ can be extended to a global bound, thus completing the proof. ■

While the robustness result established in Theorem 2 allows for generic perturbations d acting on the plant dynamics as in (33), we would like now to exploit the fact that the weighted pseudoinverse $\Pi(z)$ is invariant under scaling of z. In particular, if $\Pi(z)$ is the optimal pseudoinverse for φ, i.e. $\Pi(z)\varphi = 0$, then $\Pi(z)$ is optimal for the whole subspace $\mathrm{Im}(\varphi)$. Such a feature of the output allocation based observer (13) is a further advantage compared to the injection corrected observer (7), introduced in Section II, in terms of transient performances.

To illustrate this fact, bearing in mind that the robustness result of Theorem 2 applies to any (bounded) time-varying selection of φ, let us consider a nominal selection of the bias φ with constant direction $\bar{\varphi}$ and time-varying magnitude g_k, as follows

$$\varphi_k = g_k \bar{\varphi}, \quad g_k \in \mathbb{R} \setminus \{0\} \ \forall k \in \mathbb{N}. \tag{35}$$

Due to the presence of the time-varying factor g_k, the auxiliary observer ξ_k is no longer capable to ensure convergence of $\hat{\varphi}_k$ to φ. Moreover, since the gain M of a fast observer is typically large, some overshoots are likely to arise in the estimated bias $\hat{\varphi}_k$, with a potential inaccuracy of observer (13) and the associated output allocator. This problem might be partially overcome by following the heuristic approach of filtering the estimate $\hat{\varphi}_k$ provided by (7) before this signal is fed to the observer (13) and the output allocator, in order to reduce the effect of high frequency components of the factor g_k on the computation of the optimal weights z_k. In the case where φ is constant, so that also $\hat{\varphi}$ is exponentially converging, this additional filtering stage does not destroy the cascaded argument in the proof of Theorem 1. Instead, for the case in (35), whenever gain M characterizes a fast observer, we may expect $\hat{\varphi}$ not to be too different from φ in (35) and the filtering procedure given below may be effective.

Algorithm 1 (Scaling & Filtering):

i) Project $\hat{\varphi}_k$ onto the closed unit ball $\mathbb{B}^p \cup \mathbb{S}^{p-1}$:

$$\hat{\varphi}_k^* := \hat{\varphi}_k / \max\{|\hat{\varphi}_k|, \epsilon_\varphi\},$$

where $\epsilon_\varphi > 0$ is any regularization constant.

ii) Low-pass filter the signal $\hat{\varphi}_k^*$:

$$\hat{\varphi}_k^{**} = (1-\tau)\hat{\varphi}_{k-1}^{**} + \tau\hat{\varphi}_k^*,$$

where $\tau \in (0,1)$ is a tunable filter parameter.

iii) Feed the processed signal $\hat{\varphi}_k^{**}$ to the output allocator in (13):

$$z_{k+1} \in G(z_k, \hat{\varphi}_k^{**}).$$

Due to the continuity properties of the scaling and filtering actions in Algorithm 1, combined with the above-mentioned invariance to scaling of $\Pi(z)$ and linearity (implying ISS) of the low-pass filter in item (ii), the robustness result in Theorem 2 readily extends to the estimation scheme endowed with the extensions in Algorithm 1, as stated in the following corollary of Theorem 2.

Corollary 1: Under the assumptions of Theorem 2, with a perturbed plant as in (33), the estimation scheme (7), (13), (16), (17) endowed with the scaling and filtering action of Algorithm 1 is associated with an input-to-state stable error dynamics.

The second example in Section VII-A illustrates by numerical simulations the beneficial effect of Algorithm 1 in a reasonable scenario.

V. Selection of the optimizer map G_z

Our main result, stated in Theorem 1 establishes desirable structural rejection of the bias φ when the adaptation map G_z satisfies Property 1. A possible algorithm for the selection of G_z satisfying this property is given in this section, providing an important ingredient of our design.

A. A line-search-based optimization algorithm

For wanting to prove the implication in Property 1, for a fixed φ, we focus on minimizing the cost $|\Gamma(\varphi)z|^2$ over the set $z \in \mathbb{S}^{p-1}$, by defining a suitable difference inclusion for z iteratively minimizing $|\Gamma(\varphi)z|^2$ along the projection on $\mathbb{S}^{p-1}$ of

rank-one increments of z. More specifically, denoting by $\mathbf{e}_i$, $i = 1, ..., p$, the vectors of the canonical basis of $\mathbb{R}^p$, we focus on the following optimization problem, parametrized by $z \in \mathbb{S}^{p-1}$,

$$\min_{\mathfrak{z} \in \mathbb{S}^{p-1}} \mathfrak{z}^T S(\varphi) \mathfrak{z} := \mathfrak{z}^T \Gamma^T(\varphi) \Gamma(\varphi) \mathfrak{z}, \text{ subject to} \tag{36a}$$

$$\mathfrak{z} = \frac{z + \zeta \mathbf{e}_i}{|z + \zeta \mathbf{e}_i|}, \quad \zeta \in \overline{\mathbb{R}} := [-\infty, +\infty], \tag{36b}$$

where we consider the extended real numbers $\overline{\mathbb{R}}$ for ζ, because we consider $\mathfrak{z} = \pm \mathbf{e}_i$ for the cases $\zeta = \pm\infty$, respectively (both of them providing the same value of the quadratic cost): a straightforward extension if one rewrites (36b) as $\mathfrak{z} = \dfrac{\zeta^{-1} z + \mathbf{e}_i}{|\zeta^{-1} z + \mathbf{e}_i|}$.

The next lemma provides an explicit expression of the optimizer of (36).

Lemma 2: Fix any $i \in \{1, \dots, p\}$, define the following quantities:

$$\beta_0 := \mathbf{e}_i^T (I - z z^T) S(\varphi) z \tag{37a}$$

$$\beta_1 := \mathbf{e}_i^T S(\varphi) \mathbf{e}_i - z^T S(\varphi) z \tag{37b}$$

$$\beta_2 := z^T (\mathbf{e}_i \mathbf{e}_i^T - I) S(\varphi) \mathbf{e}_i \tag{37c}$$

Then it holds that $\gamma := \beta_1^2 - \beta_2 \beta_0 \geq 0$. Moreover, the set valued map $G_i^\star : \mathbb{S}^{p-1} \times \mathbb{R}^p \rightrightarrows \mathbb{S}^{p-1}$ defined as

$$G_i^\star(z, \varphi) := \begin{cases} \operatorname{sgn}(\beta_2) \dfrac{z\beta_2 + (\sqrt{\gamma} - \beta_1)\mathbf{e}_i}{|z\beta_2 + (\sqrt{\gamma} - \beta_1)\mathbf{e}_i|} & \text{if } \beta_2 \neq 0, \\ \dfrac{z - \frac{z^T \mathbf{e}_i}{2} \mathbf{e}_i}{(1 - \frac{z^T \mathbf{e}_i}{2})^2} & \text{if } \beta_2 = 0, \beta_1 > 0 \\ \{\pm \mathbf{e}_i\} & \text{if } \beta_2 = 0, \beta_1 \leq 0. \end{cases} \tag{37d}$$

yields optimizers for the minimization problem (36) and is outer-semicontinuous.

We are finally ready to introduce the map G_z satisfying Property 1, which stems from selecting the optimal value of all the rank-one-based optimizers $G_i^\star(z, \varphi)$, $i = 1, \dots, p$, namely

$$G_z(z, \varphi) := \operatorname*{argmin}_{\mathfrak{z} \in \{G_1^\star(z,\varphi), \dots, G_p^\star(z,\varphi)\}} \mathfrak{z}^T S(\varphi) \mathfrak{z}. \tag{37e}$$

We close this section by stating the next result, which is a fundamental ingredient for our observer design, whose proof is reported in Section V-C.

Proposition 3: Under Assumptions 1 and 2, the function G_z defined in (37e) satisfies Property 1.

Remark 2: The computational complexity of the proposed optimization algorithm (37), which consists in the explicit solution to a multiple line-search, is $O(p)$ where p is the dimension of the redundant output. In this sense, the algorithm is suitable for real-time implementation as its complexity scales linearly with the number of outputs, irrespectively of the number of states. Furthermore, at each iteration of the algorithm, the optimizer is selected among a finite number of candidates that are expressed in the closed-form (37d). ∘

B. Proof of Lemma 2

Before proceeding with the proof of Lemma 2, we state and prove the following fact, pertaining outer semicontinuous properties of optimizers.

Fact 1: Let function $\psi : \mathbb{R}^p \times \mathbb{R}^s \to \mathbb{R}$ be continuous and let $\mathcal{K} : \mathbb{R}^p \rightrightarrows \mathbb{R}^s$ be an outer semicontinuous and locally bounded set-valued mapping with nonempty values. Then the set-valued mapping $\mathcal{Q} : \mathbb{R}^p \rightrightarrows \mathbb{R}^s$ defined by

$$\mathcal{Q}(\vartheta) = \arg \min_{\mathfrak{z} \in \mathcal{K}(\vartheta)} \psi(\vartheta, \mathfrak{z}) \tag{38}$$

has nonempty values and is outer semicontinuous and locally bounded.

Proof of Fact 1. The result follows from [34, Theorem 1.17], parts of which are restated in the language of set-valued mappings in [34, Example 5.22] (see also [35, Thms 3B.3, 3B.5]). Indeed, the function $f_{\mathcal{K}} : \mathbb{R}^p \times \mathbb{R}^s \to \mathbb{R} \cup \{\infty\}$ defined by $f_{\mathcal{K}}(\vartheta, \mathfrak{z}) = \psi(\vartheta, \mathfrak{z})$ if $\mathfrak{z} \in \mathcal{K}(\vartheta)$, $f_{\mathcal{K}}(\vartheta, \mathfrak{z}) = \infty$ otherwise, is lower semicontinuous, because f is continuous and $\mathcal{K}$ is outer semicontinuous, and level-bounded in $\mathfrak{z}$, locally uniformly in ϑ, because $\mathcal{K}$ is locally bounded. Thus, [34, Theorem 1.17] applies. In fact, nonemptiness of $\mathcal{Q}(\vartheta)$ is elementary, as a continuous function $\mathfrak{z} \mapsto \psi(\vartheta, \mathfrak{z})$ is minimized over the compact set $\mathcal{Q}(\vartheta)$, and so is local boundedness of $\mathcal{Q}$ because $\mathcal{Q}(\vartheta) \subset \mathcal{K}(\vartheta)$. Since $\mathcal{Q}(\vartheta) \neq \emptyset$ and f is continuous, the function $m(\vartheta) := \min_{\mathfrak{z} \in \mathcal{K}(\vartheta)} \psi(\vartheta, \mathfrak{z})$ is continuous, by [34, Theorem 1.17 (c)]. Then, [34, Theorem 1.17 (b)] implies outer semicontinuity of $\mathcal{Q}$. ■

Let us now proceed with the proof of Lemma 2. Expanding γ yields

$$\begin{aligned}\gamma \ &= (\mathbf{e}_i^T S(\varphi)\mathbf{e}_i)^2 + (z^T S(\varphi)z)^2 - 2(\mathbf{e}_i^T S(\varphi)\mathbf{e}_i)(z^T S(\varphi)z) \\ &-(z^T(\mathbf{e}_i\mathbf{e}_i^T - I)S(\varphi)\mathbf{e}_i)(\mathbf{e}_i^T(I - zz^T)S(\varphi)z)\end{aligned}$$

Using the simplified notation $a := \mathbf{e}_i^T S(\varphi)\mathbf{e}_i$, $b := z^T S(\varphi)z$, $c := z^T S(\varphi)\mathbf{e}_i$, $d := z^T\mathbf{e}_i$ with $|d| < 1$ because $z, \mathbf{e}_i \in \mathbb{S}^{p-1}$, after some algebraic manipulations, the expression of γ reads as

$$\gamma = a^2 + b^2 + c^2 - 2ab - dbc - dac + d^2ab.$$

Using the trivial identities

$$\begin{aligned}&a^2 = \frac{d^2a^2}{2} + \left(1 - \frac{d^2}{2}\right)a^2, \quad b^2 = \frac{d^2b^2}{2} + \left(1 - \frac{d^2}{2}\right)b^2, \\ &c^2 = \frac{c^2}{2} + \frac{c^2}{2},\end{aligned}$$

the terms appearing in γ can be arranged as $\gamma = \gamma_1 + \gamma_2 + \gamma_3$ with

$$\begin{aligned}\gamma_1 \ &:= \frac{d^2a^2}{2} + \frac{c^2}{2} - dac = \left(\frac{da}{\sqrt{2}} - \frac{c}{\sqrt{2}}\right)^2 \geq 0 \\ \gamma_2 \ &:= \frac{d^2b^2}{2} + \frac{c^2}{2} - dbc = \left(\frac{db}{\sqrt{2}} - \frac{c}{\sqrt{2}}\right)^2 \geq 0 \\ \gamma_3 \ &:= \left(1 - \frac{d^2}{2}\right)(a^2 + b^2) + (d^2 - 2)ab \\ &= \left(1 - \frac{d^2}{2}\right)(a - b)^2 \geq 0,\end{aligned}$$

thus showing that the claimed condition $\gamma \geq 0$ holds true.

Let us now show that (37d) always returns minimizers. To this end, denote by $f(\zeta)$ the function optimized in (36a) subject to (36b). Differentiating with respect to ζ yields

$$f'(\zeta) = \frac{\beta_2\zeta^2 + 2\beta_1\zeta + \beta_0}{|z + \zeta\mathbf{e}_i|^4}. \tag{39}$$

Consider first the case where $z \neq \pm\mathbf{e}_i$, so that the denominator in (39) is never zero. When $\beta_2 \neq 0$, the zeros of f' are given by

$$\zeta_\pm = \frac{-\beta_1 \pm \sqrt{\gamma}}{\beta_2} \tag{40}$$

We show below that, in this case of $\beta_2 \neq 0$ and due to (40), the minimum of $f(\zeta)$ is achieved for $\zeta = \zeta_+$.

In fact, first notice that $f(+\infty) = f(-\infty) = \mathbf{e}_i^T\Gamma^T(\varphi)\Gamma(\varphi)\mathbf{e}_i$, so that the minimum must occur at some finite stationary point. For $\beta_2 > 0$ the numerator of $f'(\zeta)$ in (39) is a convex parabola whose farthest right root must be the unique minimizer, because the function is decreasing (f' is negative) between the two roots). In fact, the right root coincides with ζ_+. Conversely, for $\beta_2 < 0$, the numerator of f' is a concave parabola so that the unique minimizer of $f(\zeta)$ corresponds to farthest left root (the function f is increasing between the two roots), this being again ζ_+ in this case. Evaluating (36b) for $\zeta = \zeta_+$ yields the top expression at the right-hand side of (37d).

When instead $\beta_2 = 0$ and $\beta_1 > 0$, the numerator of $f'(\zeta)$ is a line with positive slope and so the only stationary point of $f(\zeta)$ is a minimum, given by

$$\zeta = -\frac{\beta_0}{2\beta_1} \tag{41}$$

and thus proving that the middle condition in (37d) characterizes the unique minimizer. On the other hand, when $\beta_2 = 0$ and $\beta_1 < 0$, the function $f(\zeta)$ has no minima and the $\inf$ is approached as $\zeta \to \pm\infty$, which proves that all the minimizers are characterized by the set-valued optimality condition at the third line of (37d).

Let us now address the degenerate case $\beta_1 = \beta_2 = 0$. By the definition in (37b), we have $\mathbf{e}_i^T S(\varphi)\mathbf{e}_i = z^T S(\varphi)z$, which can be substituted in (37c) to show that, with $\beta_1 = 0$, we have $\beta_0 = -\beta_2 = 0$. Therefore, $f'(\zeta) \equiv 0$, thus showing in turn that the function being optimized is actually constant in this case. In particular the vectors $\{\pm\mathbf{e}_i\}$, corresponding to picking $\zeta = \pm\infty$ in (36b), are eligible minimizers and the bottom option in (37d) is consistent.

The last case to be considered is $z = \pm\mathbf{e}_i$, which also leads to $\beta_0 = \beta_1 = \beta_2 = 0$, and for which the only attainable values for $\mathfrak{z}$ in (36b) are $\pm\mathbf{e}_i$, both of them leading to the cost $z^T S(\varphi)z$, therefore both of them being minimizers, as characterized in the third line of (37d).

To prove outer semi-continuity of the map $(z,\varphi)\mapsto G_i^\star(z,\varphi)$ defined in (37d), let us first observe that whenever $z\neq\pm\mathbf{e}_i$ the feasible set in optimization (36) is the intersection of $\mathbb{S}^{p-1}$ with the half plane containing the line $\mathcal{L}(z):=\{z+\zeta\mathbf{e}_i:\zeta\in(-\infty,+\infty)\}$ and the origin (the origin does not belong to $\mathcal{L}(z)$ because $z\neq\pm\mathbf{e}_i$):

$$\mathfrak{z}\in\mathcal{P}(z):=\left\{\frac{z+\zeta\mathbf{e}_i}{|z+\zeta\mathbf{e}_i|},\zeta\in[-\infty,\infty]\right\}.$$

Since $\mathcal{L}$ is a continuous function of z, so is also $\mathcal{P}$.

Now we apply Fact 1 two times as follows. First, with $\vartheta=(z,\varphi)$, select $\psi_1(\vartheta,\mathfrak{z})=\mathfrak{z}^TS(\varphi)\mathfrak{z}$, whose continuity is trivial, and select $\mathcal{K}_1$ as

$$\mathcal{K}_1(\vartheta)=\begin{cases}\mathbb{S}^{p-1}, & \text{if } \beta_1(\vartheta)=\beta_2(\vartheta)=0,\\ \mathcal{P}(z), & \text{otherwise,}\end{cases}\tag{42}$$

where we explicitly indicated the dependence on ϑ of β_1 and β_2 in (37b), (37c). The set-valued map $\mathcal{K}_1$ in (42) is globally bounded (it is a subset of the unit sphere $\mathbb{S}^{p-1}$) and outer semi-continuous because it coincides with the continuous map $\mathcal{P}$ almost everywhere, and corresponds to the whole (closed) set $\mathbb{S}^{p-1}$ in the closed set where $\beta_1(\vartheta)=\beta_2(\vartheta)=0$ (as established in [33, Lemma 5.10], outer semi-continuity coincides with a map having a closed graph). With the selections above, due to Fact 1, the map $\mathcal{Q}_1(\vartheta)=\arg\min_{\mathfrak{z}\in\mathcal{K}_1(\vartheta)}\mathfrak{z}^TS(\varphi)\mathfrak{z}$ is outer semi-continuous and, due to the proof of optimality stated above, coincides with the map $\vartheta\mapsto G_i^\star(\vartheta)$ defined in (37d) everywhere, except for the points where $\beta_1(\vartheta)=\beta_2(\vartheta)=0$.

Let us now apply again Fact 1 as follows. Define

$$\mathcal{K}_2(\vartheta)=\begin{cases}\mathbb{S}^{p-1}, & \text{if } \beta_1(\vartheta)=\beta_2(\vartheta)=0,\\ \mathcal{Q}_1(\vartheta), & \text{otherwise,}\end{cases}\tag{43}$$

which is once again outer semi-continuous because it is globally bounded and has a closed graph. Applying again Fact 1 with the continuous selection $\psi(\vartheta,\mathfrak{z})=1-|\mathfrak{z}^T\mathbf{e}_i|$, we obtain that map $\mathcal{Q}_2(\vartheta)=\arg\min_{\mathfrak{z}\in\mathcal{K}_2(\vartheta)}1-|\mathfrak{z}^T\mathbf{e}_i|$ is outer semi-continuous. Moreover, $\mathcal{Q}_2(\vartheta)=\mathcal{Q}_1(\vartheta)=G_i^\star(\vartheta)$ everywhere except for the points where $\beta_1(\vartheta)=\beta_2(\vartheta)=0$. Let us now analyze these remaining points. Since

$$\beta_1(\vartheta)=\beta_2(\vartheta)=0\ \Rightarrow\ \mathcal{K}_2(\vartheta)=\mathbb{S}^{p-1},$$

then the optimizer of $\psi(\vartheta,\mathfrak{z})=1-|\mathfrak{z}^T\mathbf{e}_i|$ is clearly $\mathcal{Q}_2(\vartheta)=\pm\mathbf{e}_i$, which coincides with the selection of $G_i^\star(\vartheta)$ at the third line of (37d). This means that $\mathcal{Q}_2(\vartheta)=G_i^\star(\vartheta)$ also when $\beta_1(\vartheta)=\beta_2(\vartheta)=0$ and outer semi-continuity of $\mathcal{Q}_2$ implies outer semi-continuity of $G_i^\star$, as to be proven. ■

Remark 3: Based on the proof of Lemma 2, it is possible to give a qualitative characterization of the extrema of (36) in the various cases considered in (37d). In fact, when $\beta_2\neq0$ the function admits both a global minimum and a global maximum. When $\beta_2=0$ and $\beta_1>0$, the function still admits a global minimum, whereas its maximum is formally attained at $\zeta=\pm\infty$ (note that the cost is the same for $\zeta=+\infty$ and $\zeta=-\infty$). In the complementary scenario $\beta_2=0$ and $\beta_1<0$, a mirror property holds with the minimum attained at $\zeta=\pm\infty$. In all three cases, the minimization problem is nontrivial and minima are strict. Conversely, in the limit case $\beta_2=\beta_1=0$ (which implies $\beta_0=0$), the function (36a) reduces to a constant, due to (39) and the optimization problem (36) becomes trivial. In particular, such degenerate condition only arises when $z=\pm\mathbf{e}_i$ or, more generally, when z and $\mathbf{e}_i$ belong to a common eigenspace for the matrix $S(\varphi)$.

C. Proof of Proposition 3

Before proceeding with the proof of Proposition 3, we introduce the following lemma, hinging on the properties of Y in Assumption 2.

Lemma 3: Let $Y\in\mathbb{R}^{p\times q}$ satisfy Assumption 2, denote $S=\mathrm{diag}(\varphi)YY^T\mathrm{diag}(\varphi)$ as in (36a), and $\lambda_{\min}:=\min\sigma(S)\backslash\{0\}>0$. Then

$$\min_{j=1,\dots,p}\mathbf{e}_j^TS\mathbf{e}_j<\lambda_{\min}.\tag{44}$$

Proof: Define $\Sigma=Y^T\mathrm{diag}(\varphi)^2Y\in\mathbb{R}^{q\times q}$, and observe that

$$\sigma(\Sigma)\setminus\{0\}=\sigma(S)\setminus\{0\}.\tag{45}$$

Since YY^T is a projection and the non-alignment condition in item 2 of Assumption 2 holds[2], then one has

$$\mathbf{e}_j^TYY^T\mathbf{e}_j<1\tag{46}$$

$$\mathbf{e}_j^TS\mathbf{e}_j=\varphi_j^2\mathbf{e}_j^TYY^T\mathbf{e}_j\leq\varphi_j^2,\tag{47}$$

[2]It is easy to check that $\mathbf{e}_j^TYY^T\mathbf{e}_j=1\ \Leftrightarrow\ \mathbf{e}_j\in\mathrm{Im}(Y)$

where the equality in (47) holds if and only if $\varphi_j = 0$. Now, let $(\bar{\lambda}, b)$ be an arbitrary eigenpair for Σ with $\bar{\lambda} > 0$. Then, using (46) and item 1 of Assumption 2, one has

$$b^T \Sigma b = b^T (Y^T \mathrm{diag}(\varphi)^2 Y) b = \bar{\lambda} b^T b = \bar{\lambda} b^T Y^T Y b,$$

which is equivalent to

$$b^T Y^T \underbrace{\left(\mathrm{diag}(\varphi)^2 - \bar{\lambda} I_{p\times p}\right)}_{=:N} Y b = 0.$$

Since by construction $Yb \neq 0$, the only way for the latter to be satisfied is N being either singular or sign indefinite, which, together with $\bar{\lambda} > 0$, results in

$$\bar{\lambda} \geq \min_{j=1,\dots,p} \varphi_j^2. \tag{48}$$

The latter holds for each non-zero eigenvalue $\bar{\lambda}$ of Σ, hence also for each non-zero eigenvalue $\bar{\lambda}$ of S, in view of (45).

Now, two cases should be considered: either (i) $\min_{j=1,\dots,p} \varphi_j^2 > 0$, which means that the right inequality in (47) is strict, so that combining it with (48) we obtain (44), or (ii) $\min_{j=1,\dots,p} \varphi_j^2 = 0$, which means (from positivity of $\lambda_{\min}$) that $\lambda_{\min} > \min_{j=1,\dots,p} \varphi_j^2$ and the result (44) is proven again, due to (47), thus concluding the proof. ■

Based on Lemma 3, we are now ready to prove Proposition 3.

Proof of Proposition 3. We first prove the properties of G_z, and then we prove the decrease condition (22).

The map $G_z(z, \varphi)$ in (37e) is defined through the minimum over a finite set of outer semi-continuous maps and therefore it is an outer semi-continuous map itself. Moreover, it is trivially nonempty because $G_i^\star$ is never empty, and globally bounded because its values belong to the compact set $\mathbb{S}^{p-1}$.

Let us now prove the decrease condition (22). First note that the optimal cost in (36a) coincides with $|\Gamma(\varphi) z^+|^2$. Using optimality of G_z in (37e), let us first address the case where $\beta_0 \neq 0$ for at least one $i \in \{1, \dots, p\}$. Under this condition, we prove next that $z \notin G_i^\star(z, \varphi)$ by also leveraging on the observations reported in Remark 3. Indeed, consider all three cases in (37d).

• In the first case, the minimizer $\mathfrak{z}^\star$ of (36) is obtained by selecting $\zeta = \zeta_+$ (see (40)): the unique minimum of $\mathfrak{z}^T S(\varphi) \mathfrak{z}$; since $\beta_2 \neq 0$, then $\zeta_+ \neq 0$ and $z \neq \mathfrak{z}^\star$ so that $z \notin G_i^\star(z, \varphi)$.

• In the second case, the unique minimizer is ζ as in (41), which is once again not zero, and again we have $z \notin G_i^\star(z, \varphi)$.

• In the third case, first note that it should be $\beta_1 < 0$, because $\beta_2 = \beta_1 = 0$ would imply $\beta_0 = 0$ while we are focusing on $\beta_0 \neq 0$; but $\beta_1 < 0$ implies $z \neq \pm \mathbf{e}_i$, while $\pm \mathbf{e}_i$ are the only two optimizers, as discussed in Remark 3. As a consequence, z is not an optimizer, namely $z \notin G_i^\star(z, \varphi)$.

The fact that $z \notin G_i^\star(z, \varphi)$, established above, implies condition $(|\Gamma(\varphi) z_i^\star| < |\Gamma(\varphi) z|)$ for any $z_i^\star \in G_i^\star(z, \varphi)$, due to the fact that z is not a minimizer of the underlying line-search problem (while $z_i^\star$ is a minimizer due to Lemma 2). Finally, the minimum in (37e) ensures that any $z^\star \in G_z(z, \varphi)$ leads to a value $|\Gamma(\varphi) z^\star| \leq |\Gamma(\varphi) z_i^\star|$, thus showing the decrease condition (22) in Property 2.

The condition where $\beta_0 = 0$ for all $i \in \{1, \dots, p\}$ is more challenging since a decrease of the cost function occurs if and only if $\beta_1 < 0$ for at least one $i \in \{1, \dots, p\}$ (whereas due to $\beta_0 = 0$, $z_i^\star = z$ for any $i \in \{1, \dots, p\}$ such that $\beta_1 \geq 0$). On the other hand, $\beta_0 = 0$ for all $i = 1, ..., p$ implies that $(I - zz^T) S(\varphi) z = 0$, which corresponds to z being an eigenvector of $S(\varphi)$. If the eigenvalue corresponding to the eigenvector z is zero, then $\Gamma(\varphi) z = 0$ and (the left case in) the decrease condition (22) holds. If instead the eigenvalue corresponding to the eigenvector z is some $\bar{\lambda} > 0$, then we may invoke Lemma 3, which establishes that there exists at least one search direction providing a smaller value of the cost $|\Gamma(\varphi) z^+|^2$. In other words, Lemma 3 establishes that $\beta_1 < 0$ for at least one $i \in \{1, ..., p\}$ and the decrease condition (22) of Property 1 holds also in this last case. ■

VI. Overall observation scheme

We combine here the construction in Section IV and the ensuing Theorem 1 (which relies on Assumption 1) with the algorithm design in Section V and the ensuing Proposition 3 (which relies on Assumption 2). This combination allows stating the following corollary pertaining the observation scheme represented in Figure 1 and comprising plant (1), the asymptotic bias estimator (7), the selector (17), the adaptive pseudoinverse observer (13) and the optimizer (16) with the choice of G_z in (37), which leads to the error dynamics (8), (20) derived in Section IV-A.

Corollary 2: Under Assumptions 1 and 2, consider any pair of gains M and L such that $A - LH$ and $A - MH$ are Schur. If Property 2 holds, then the compact set $\mathcal{A}$ in (25) is globally asymptotically stable for the error dynamics (8), (20) associated with the plant-observer scheme (1), (7), (17), (13), (16), (37).

Corollary 2 clarifies that the only requirement to be clarified for the effectiveness of the proposed observation scheme stands in Property 2, which is associated with a nontrivial interplay between the bias φ and the output matrix C, as characterized by the matrix Y. An interesting defective case providing a necessary condition involving φ and Y corresponds to the scenario

of two identical sensors sharing the same exact bias, which structurally prevents our idea from being applicable. This specific case, and its generalization, is characterized in the next remark.

Remark 4: In the special case where $\varphi_o = 0$ in (6), namely $\varphi \in \mathrm{Im}(Y)$, it is impossible to find a vector z such that $R(z)$ is invertible and $\Gamma(\varphi)z = \Gamma(z)\varphi = 0$. To see this, since from (6) we get $\varphi = Yw_\varphi$ for some $w_\varphi \in \mathbb{R}^q$, one has

$$R(z)^{-1}\Gamma(z)\varphi = (Y^T \operatorname{diag}(z)Y)^{-1}Y^T \operatorname{diag}(z)Yw_\varphi = w_\varphi,$$

which implies that the effect of φ (through w_φ) cannot be filtered out structurally by the adaptive pseudo-inverse. ∘

Besides the necessary conditions for Property 2 discussed in Remark 4, we instead discuss below two relevant applications of our results: a first one, requires having one direction of redundancy, namely $p - q = 1$ in Assumption 1, which allows proving Property 2; a second one where, with general redundancy level, we propose an extended scheme overcoming the need for Property 2 with the drawback of potential reduced effectiveness of the proposed nonlinear observation scheme.

A. The 1-redundancy case

We consider here the case where we impose the next 1-redundancy assumption.

Assumption 3: The integers p (size of y) and q (rank of C) in Assumption 1 satisfy $p - q = 1$.

When enforcing Assumption 3, we have the advantage that matrix $\Gamma(\varphi)$ has dimension $p - 1 \times p$ and we may characterize the case where its kernel has dimension 1. Indeed, the least dimension of the kernel coincides with the redundancy level $p-q$, therefore this strategy only applies to the 1-redundancy case.

The proposition below formalizes a convenient characterization of scenarios where Property 2 holds, based on the next technical assumption, which involves easily checkable conditions on φ and Y.

Assumption 4: For matrix Y and vector φ it holds that $\det(Y^T \operatorname{diag}(\varphi)^2 Y) \neq 0$ and there exists $j \in \{1, \dots, p\}$ such that $\det(Y^T \operatorname{diag}(n_j(\varphi))Y) \neq 0$, where $n_j(\varphi) = \Xi(\varphi)\mathbf{e}_j$ and

$$\Xi(\varphi) = I - \operatorname{diag}(\varphi)Y \left(Y^T \operatorname{diag}(\varphi)^2 Y\right)^{-1} Y^T \operatorname{diag}(\varphi). \tag{49}$$

Proposition 4: Under Assumptions 3 and 4, Property 2 holds for a sufficiently small $\epsilon > 0$.

Proof: First note that having $\det(Y^T \operatorname{diag}(\varphi)^2 Y) \neq 0$ from Assumption 4 implies that $\Gamma(\varphi)$ is full row rank. Therefore, its kernel is one-dimensional and coincides with the image of the projection matrix $\Xi(\varphi)$ in (49), which is by construction a rank 1 matrix. Then, any of the nonzero columns $n_j(\varphi)$ of $\Xi(\varphi)$, as denoted in Assumption 4 is a basis vector spanning the one-dimensional subspace $\mathcal{Z}^\dagger := \{z \in \mathbb{R}^p : \Gamma(z)\varphi = 0\}$. Introduce the singularity set

$$\mathcal{Z}_{\text{bad}} := \{z \in \mathbb{R}^p : \det(R(z)) = 0\}, \tag{50}$$

which by construction is a $p-1$ dimensional cone. Due to the fact that $\mathcal{Z}^\dagger$ has dimension 1, one and only one of the following two conditions is fulfilled:

$$\text{(i)} \left[\mathcal{Z}^\dagger \subset \mathcal{Z}_{\text{bad}}\right] \quad \text{OR} \quad \text{(ii)} \left[\mathcal{Z}^\dagger \cap \mathcal{Z}_{\text{bad}} = \{0\}\right], \tag{51}$$

i.e., either the kernel $\mathcal{Z}^\dagger$ is entirely contained in the singularity set (50) or it is everywhere away from it, except at the origin. On the other hand, case (i) can be ruled out by the second requirement in Assumption 4, entailing that the spanning vector of $\mathcal{Z}^\dagger$ does not belong to the singularity set $\mathcal{Z}_{\text{bad}}$ in (50). Now, observing that $\mathcal{Z}^\star = \mathcal{Z}^\dagger \cap \mathbb{S}^{p-1} = \{z_\circ, -z_\circ\}$ for some $z_\circ \in \mathbb{S}^{p-1}$ and using condition (ii) in (51), a strictly positive number $\bar{r} > 0$ exists, such that

$$|\det(R(\pm z_\circ))| = \bar{r}.$$

Picking $\epsilon < \bar{r}$, the pair of antipodal points $\{z_\circ, -z_\circ\}$ belong to the interior of $\mathcal{S}_\epsilon$, thus showing that Property 2 holds in this case. ■

We may now state the following corollary of Corollary 2 and Proposition 4.

Corollary 3: Under Assumptions 1, 2, 3 and 4, consider any pair of gains M and L such that $A - LH$ and $A - MH$ are Schur. Then the compact set $\mathcal{A}$ in (25) is globally asymptotically stable for the error dynamics (8), (20) associated with the plant-observer scheme (1), (7), (17), (13), (16), (37).

B. Generalized scheme with a logic variable

We discuss here the case where no assumption is imposed on φ nor on the level of output redundancy, to show that our scheme remains well behaved, even though the structural rejection of φ cannot be always guaranteed as in the previous section. The idea of this section is to propose a modified scheme that exploits the knowledge of the situations where the selector map in (17) disregards z and sticks to the previous value of s, to activate an injection term in the observer dynamics.

To this end, we first introduce a logic state variable $h \in \{0,1\}$ in our observation scheme, and then modify the selector (17) as follows:

$$\begin{bmatrix} s^+ \\ h^+ \end{bmatrix} \in G_h(s,z) := \begin{cases} \left[\begin{smallmatrix} z \\ 0 \end{smallmatrix}\right] & \text{if } z \notin \overline{\mathbb{S}^{p-1} \setminus \mathcal{S}_\epsilon}, \\ \left[\begin{smallmatrix} s \\ 1 \end{smallmatrix}\right] & \text{if } z \notin \mathcal{S}_\epsilon, \\ \left\{\left[\begin{smallmatrix} s \\ 1 \end{smallmatrix}\right], \left[\begin{smallmatrix} z \\ 0 \end{smallmatrix}\right]\right\} & \text{otherwise.} \end{cases} \tag{52}$$

With the logic-enhanced selector (52), variable h is an indicator of whether the adaptation parameter z is being transferred to s (in that case we have $h = 0$) or the variable s is kept constant, possibly away from the desirable set where the bias φ is suitably rejected. Motivated by this second case, variable $h = 1$ is used to trigger an additive term in the observer dynamics (13), which is extended as follows

$$\begin{aligned} \hat{x}^+ &= A\hat{x} + Bu + L\Pi(s)(y - \hat{y} - h\hat{\varphi}) \\ \hat{y} &= C\hat{x}. \end{aligned} \tag{53}$$

The resulting h-modified observation scheme, referred to as adaptive pseudo-inverse observer with *residual injection*, comprises the dynamics (1), (7), (52), (53), (16), (37) associated with the error dynamics (8) combined with the following generalization of the error dynamics (20)

$$\begin{aligned} e^+ &= (A - LH)e + LR(s)^{-1}\Gamma(s)(\varphi - h\hat{\varphi}), \\ \begin{bmatrix} s^+ \\ h^+ \end{bmatrix} &\in G_h(s,z), \qquad\qquad (e,s,h,z) \in \mathcal{E}_h, \\ z^+ &\in G_z(z,\hat{\varphi}), \end{aligned} \tag{54}$$

with $\mathcal{E}_h := \mathbb{R}^n \times \mathcal{S}_\epsilon \times \{0,1\} \times \mathbb{S}^{p-1}$ being the (forward invariant) set where the state (e,s,h,z) is allowed to evolve, and with the input $\hat{\varphi} \in \mathbb{R}^p$ coming from observer (7).

The effect of the term $h\hat{\varphi}$ on the dynamics of e in (54) is that two cases can occur: either $h = 0$ for a finite number of times, and then the dynamics eventually is forced by the perturbation $\varphi - \hat{\varphi}$, which converges to zero due to the properties of the asymptotic bias estimator, or $h = 0$ for an infinite number of times, which implies that s converges to z and the reduction argument of Theorem 1 holds, so that convergence to zero of e is guaranteed. Combining these two cases, we may prove that the logic-enhanced scheme establishes global asymptotic stability of the compact set

$$\begin{aligned} \mathcal{A}_h := \{(\varepsilon, e, s, h, z) \in \mathbb{R}^n \times \mathbb{R}^n \times \mathcal{S}_\epsilon \times \{0,1\} \times \mathbb{S}^{p-1} : \\ \varepsilon = \varepsilon^\star, e = 0\}, \end{aligned} \tag{55}$$

without the need of enforcing Property 2. This fact is formalized in the next corollary.

Corollary 4: Under Assumptions 1 and 2, consider any pair of gains M and L such that $A - LH$ and $A - MH$ are Schur. Then the compact set $\mathcal{A}_h$ in (55) is globally asymptotically stable for the error dynamics (8), (54) associated with the plant-observer scheme (1), (7), (52), (53), (16), (37).

Note that, Corollary 4 does not imply that solutions asymptotically approach the set where $\Gamma(s)\varphi = 0$, because a generic value of $s \in \mathcal{S}_\epsilon$ is allowed for s in $\mathcal{A}_h$ of (55). Nevertheless, we emphasize that whenever z approaches a point in the interior of $\mathcal{S}_\epsilon$, which is therefore feasible for s, the variable q eventually remains identically zero and the solutions of the logic-enhanced scheme coincide with those of the original scheme in Corollary 2. As a consequence, one can think of the enhanced scheme of this section as a clever solution recovering the behavior established in Corollary 2 whenever Property 2 holds, and also leading to asymptotic estimation via adaptive pseudoinverses in the absence of Property 2. In particular, as discussed later in Section VII.B, the modified scheme (54) is likely to provide better performances than a scheme with a static pseudo-inverse having fixed weights.

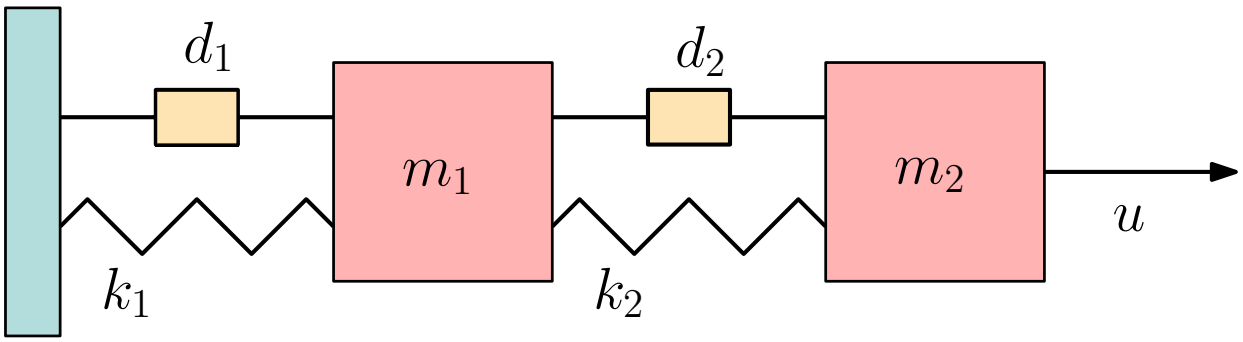

Fig. 2. Coupled mass-spring-damper systems

VII. Numerical simulations

Let us illustrate by means of numerical simulations the potential of the dynamic output allocation method. We consider the case-study of coupled mass-spring-damper subsystems as in Figure 2, whose (continuous-time) state-space representation is

$$\begin{bmatrix}\dot{x}_1\\ \dot{x}_2\\ \dot{x}_3\\ \dot{x}_4\end{bmatrix} = \underbrace{\begin{bmatrix} 0 & 0 & 1 & 0\\ 0 & 0 & 0 & 1\\ -\frac{k_1+k_2}{m_1} & \frac{k_2}{m_1} & -\frac{d_1+d_2}{m_1} & \frac{d_2}{m_1}\\ \frac{k_2}{m_2} & -\frac{k_2}{m_2} & \frac{d_2}{m_2} & -\frac{d_2}{m_2}\end{bmatrix}}_{=A_0}\begin{bmatrix}x_1\\ x_2\\ x_3\\ x_4\end{bmatrix} + \underbrace{\begin{bmatrix}0\\0\\0\\ \frac{1}{m_2}\end{bmatrix}}_{=B_0} u.$$

By applying an exact discretization procedure with sampling time $\tau > 0$, we get a discrete-time system in compact form

$$x^+ = Ax + Bu,$$

with $A = \exp(A_0\tau)$ and $B = \int_0^\tau \exp(A_0(\tau-\sigma))B_0 d\sigma$. The system parameters for the simulation study have been chosen according to Table I.

m_1	m_2	k_1	k_2	d_1	d_2	τ
1.5	1	1.2	1	$5{\cdot}10^{-3}$	$9{\cdot}10^{-3}$	10^{-2}
[Kg]	[Kg]	[N/m]	[N/m]	[Ns/m]	[Ns/m]	[s]

TABLE I
System parameters used in the simulations.

The system is supposed to be controlled by an open-loop periodic input u. To better highlight the features of the proposed architecture, two different sensor combinations have been considered, falling into the 1-redundancy case and the general case, respectively.

A. First scenario: p = 3, q = 2

We begin by considering the system equipped with three sensors, providing: two position measurements for the displacements of the mass m_1 and the mass m_2, and a range measurement for the relative distance between the two masses, with respect to the first mass. Such (redundant) suite of sensors can be encoded in the output matrix

$$C = \begin{bmatrix}1 & 0 & 0 & 0\\ 0 & 1 & 0 & 0\\ 1 & -1 & 0 & 0\end{bmatrix}$$

which is the same used in Example 1. In this first scenario the unknown vector φ has been chosen as $\varphi = \gamma[1\ -1.5\ 0.5]^T$, where γ is a possibly time-varying amplitude. Taking the selection (Y, H) as described in (4a)-(4b), the conditions of Assumption 2 are met. Based on this choice, the gains of the asymptotic bias estimator and the pseudoinverse observer are selected in order to assign the eigenvalues according to

$$\operatorname{spec}(A - MH) = \{0, 0, 0.01, 0.01\},$$
$$\operatorname{spec}(A - LH) = \{0.75, 0.8, 0.85, 0.9\}$$

Two examples have been considered, with $\gamma_k = 1$ constant and with $\gamma_k = 1 + 0.1\sin(100\,\tau k)$, where k denotes the discrete time. In the first case, we compare the performance of the adaptive pseudo-inverse observer against an observer based on a constant pseudo-inverse with uniform weights, corresponding to the choice $s \equiv \frac{1}{\sqrt{3}}\mathbb{1}$. The behavior of the estimation error $|x - \hat{x}|$ is shown in Figure 3 (top), where the vanishing of the bias effect thanks to the adaptation law can be appreciated (see the zoomed box). It must be noticed that, due to the adaptation, the dynamic pseudo-inverse observer is likely to experience a larger transient. The evolution of the selector s is reported in Figure 3 (bottom). In this case, where Assumptions 3 and 4 hold, the selector s coincides with the optimizer z, thus guaranteeing the optimal adaptation of the pseudoinverse $\Pi(s) = \Pi(z)$ and a perfect cancellation of $\Pi(s)\hat{\varphi}$, in light of Corollary 3.

In the second case with non constant γ, considering a larger number of samples to allow for a correct filtering action, we have enhanced the proposed adaptive observer with the scaling & filtering algorithm described in Section IV-D. We propose in Figure 4 (top) a comparison of the performance of our adaptive observer against a standard observer with injection of the estimated $\hat{\varphi}$, defined by

$$\hat{x}^+ = A\hat{x} + Bu + L(Y^\dagger(Cx - \hat{\varphi}) - H\hat{x}), \tag{56}$$

as well as with an enhanced version of the same where the estimation $\hat{\varphi}$ is processed by a filter before the injection. The adaptive observer largely outperforms the observer (56) with injection without filtering. The comparison with the observer (56)

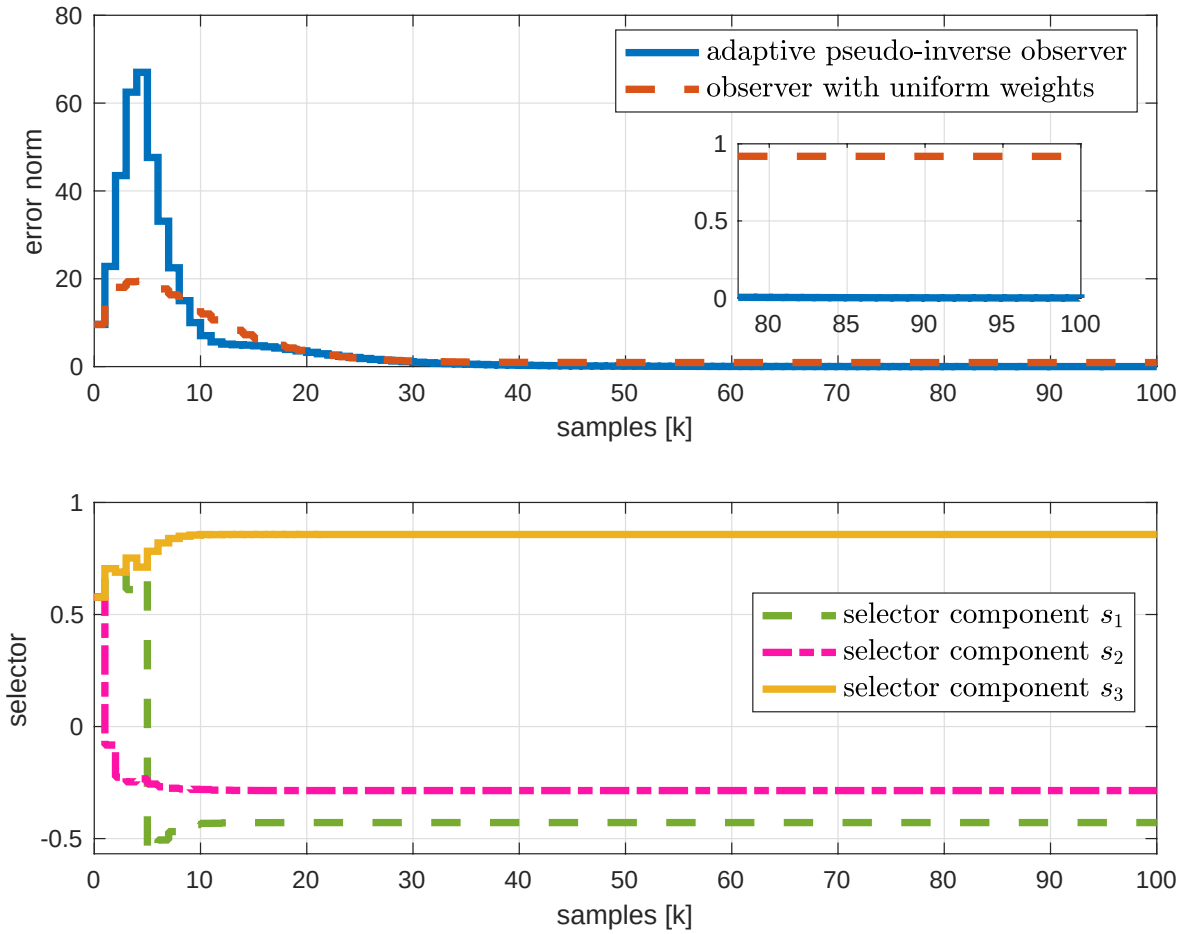

Fig. 3. Scenario 1 with constant φ: norm of estimation error (top) and selector states (bottom)

with injection of the filtered estimation $\hat{\varphi}$ is more interesting and meaningful, and one can still appreciate the improvement provided by the adaptive observer, which yields a lower steady-state estimation error. The evolution of the selector states is illustrated in Figure 4 (bottom): after an initial highly oscillatory transient, the steady state corresponds to a slight perturbation of the constant steady state of Figure 3 (bottom).

B. Second scenario: p = 4, q = 2

In this second scenario, in addition to the previous sensors, we consider another range sensor measuring the relative distance with respect between the two masses as seen by the second mass. Overall, this corresponds to dealing with the augmented output matrix

$$C = \begin{bmatrix} 1 & 0 & 0 & 0 \\ 0 & 1 & 0 & 0 \\ 1 & -1 & 0 & 0 \\ -1 & 1 & 0 & 0 \end{bmatrix}$$

for which a decomposition $C = YH$ with the desired property can be easily obtained as in the previous case. The vector φ is now supposed to be constant and equal to $\varphi = [1 \ \ -1.5 \ 0.5 \ \ -0.15]^T$. Due to the condition $p = 4 > 2 = q$, we might expect the intersection $\mathcal{Z}^\star \cap \mathcal{Z}_{\text{bad}}$ to be nonempty and, for this reason, we implement the modified scheme with residual injection described in Section VI-B and defined by (53)-(54). The corresponding estimation error is depicted in Figure 5 (top), showing that asymptotic convergence is achieved and proving the advantage of the proposed scheme against an observer designed using the pseudo-inverse with constant uniform weights, namely with $s \equiv \frac{1}{2}\mathbb{1}$. For the sake of completeness also the comparison with the adaptive observer without residual injection is considered. The selector state is prevented from coinciding with the optimizer state, as evident from Figure 5 (bottom), because the latter lies too close to the singularity region $\mathcal{Z}_{\text{bad}}$ and Property 2 does not hold in this case. Due to such condition, the adaptive observer without residual injection, whose evolution is also

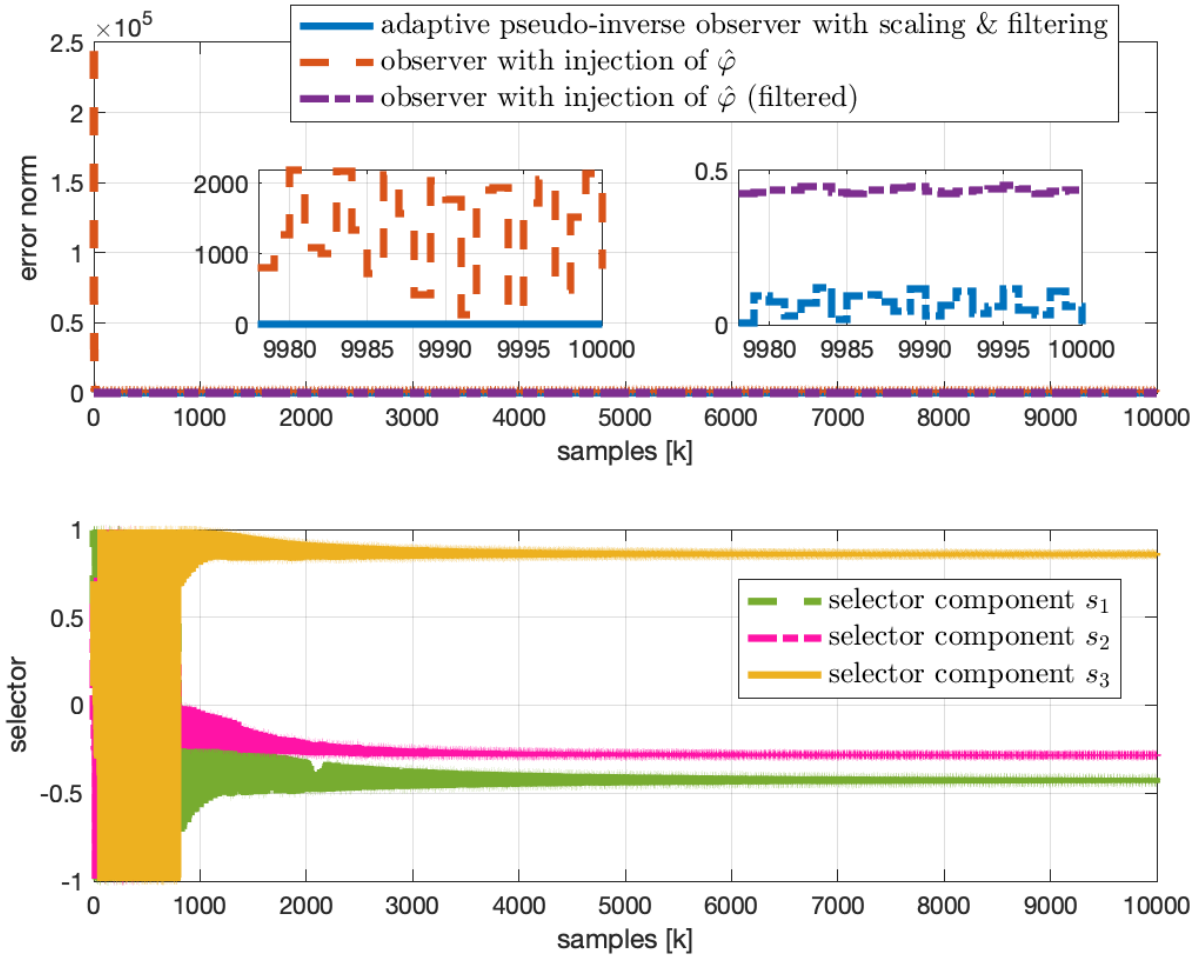

Fig. 4. Scenario 1 with time-varying φ: norm of estimation error (top) and selector states (bottom)

depicted in Figure 5 (top), is not able to deliver an accurate estimate, thus confirming the benefit of the modified scheme (53)-(54).

VIII. Conclusions

A robust estimation scheme has been proposed based on adaptive pseudoinverses with dynamic weights coupled with linear Luenberger-like observers in the presence of redundant measurements for discrete-time linear systems. The proposed architecture, which is based on the cascade interconnection of two different observers, is proved to be successful at rejecting constant biases affecting the sensor measurements without the need of matching conditions or any prior knowledge on the structure of the perturbations. The first observer is in charge of estimating the output perturbation signal, whereas the second uses dynamic pseudoinverses to seek for the best combination of sensors. Such an optimization scheme hinges on a novel line-search algorithm for the minimization of positive semi-definite quadratic forms over the unit sphere. In addition, a selector is introduced to overrule the optimizer whenever this would drive the adaptive pseudo-inverse too close to singularity.

Extensive simulations illustrate and corroborate the theoretical findings, exploiting several key aspects of the proposed method through the application to the case study of a discrete-time mechanical system with redundant sensors.

Future work will be oriented towards obtaining a global, or semiglobal, solution for the continuous-time case, possibly introducing hybrid optimization policies based on the results contained in this paper. Moreover, we are currently working on the application of our line-optimization algorithm to other problems such as calibration of cameras and attitude estimation. Finally, it may be worth investigating the extension of the proposed design scheme to unknown input observers with redundant outputs.

Acknowledgements

The authors would like to thank Rafal Goebel for his suggestions related to Fact 1 and the ensuing proof of outer semi-continuity of the map G_i^* in (37).

REFERENCES

[1] T. A. Johansen and T. I. Fossen, "Control allocation: A survey," *Automatica*, p. in press, 2013.
[2] L. Zaccarian, "Dynamic allocation for input redundant control systems," *Automatica*, vol. 45, pp. 1431–1438, 2009.
[3] W. C. Durham, "Constrained control allocation," *J. of Guidance, Control and Nav.*, vol. 16, pp. 717–725, 1993.
[4] M. Bodson, "Evaluation of optimization methods for control allocation," *J. of Guidance, Control and Nav.*, vol. 25, pp. 703–711, 2008.
[5] A. Cristofaro and S. Galeani, "Output invisible control allocation with steady-state input optimization for weakly redundant plants," in *Proc. 53rd IEEE Conf. Decision and Control*, 2014, pp. 4246–4253.
[6] J. Zhou, M. Canova, and A. Serrani, "Predictive inverse model allocation for constrained over-actuated linear systems," *Automatica*, vol. 67, pp. 267–276, 2016.
[7] A. Cristofaro, S. Galeani, and A. Serrani, "Output invisible control allocation with asymptotic optimization for nonlinear systems in normal form," in *2017 IEEE 56th Annual Conference on Decision and Control (CDC)*. IEEE, 2017, pp. 2563–2568.
[8] T. A. Lima, S. Tarbouriech, F. G. Nogueira, and B. C. Torrico, "Co-design of dynamic allocation functions and anti-windup," *IEEE Control Systems Letters*, vol. 5, no. 6, pp. 2198–2203, 2020.
[9] H. Alwi and C. Edwards, "Sliding mode FTC with on-line control allocation," *Proc. 45th IEEE Conf. on Decision and Control*, pp. 5579–5584, 2006.
[10] J. Tjønnås and T. Johansen, "Adaptive control allocation," *Automatica*, vol. 44, pp. 2754–2766, 2008.
[11] A. Casavola and E. Garone, "Fault-tolerant adaptive control allocation schemes for overactuated systems," *Int. J. Robust and Nonlinear Control*, vol. 20, pp. 1958–1980, 2010.
[12] A. Cristofaro and T. A. Johansen, "Fault-tolerant control allocation with actuator dynamics: Finite-time control reconfiguration." in *Proc. 53rd IEEE Conf. Decision and Control*, 2014, pp. 4971–4976.
[13] M. Naderi, T. A. Johansen, and A. K. Sedigh, "A fault tolerant control scheme using the feasible constrained control allocation strategy," *International Journal of Automation and Computing*, vol. 16, pp. 628–643, 2019.
[14] D. Corona and A. Cristofaro, "Some remarks on optimal output regulation for weakly dual redundant plants," in *2016 24th Mediterranean Conference on Control and Automation (MED)*, 2016, pp. 1205–1211.
[15] D. Catlin, *Estimation, control, and the discrete Kalman filter*. Springer Science & Business Media, 2012, vol. 71.
[16] R. H. Rogne, T. A. Johansen, and T. I. Fossen, "Observer and imu-based detection and isolation of faults in position reference systems and gyrocompasses with dual redundancy in dynamic positioning," in *Control Applications (CCA), IEEE Conference on*, 2014, pp. 83–88.
[17] I. Samy, I. Postlethwaite, and D. W. Gu, "Survey and application of sensor fault detection and isolation schemes," *Control Engineering Practice*, vol. 19, no. 7, pp. 658–674, 2011.

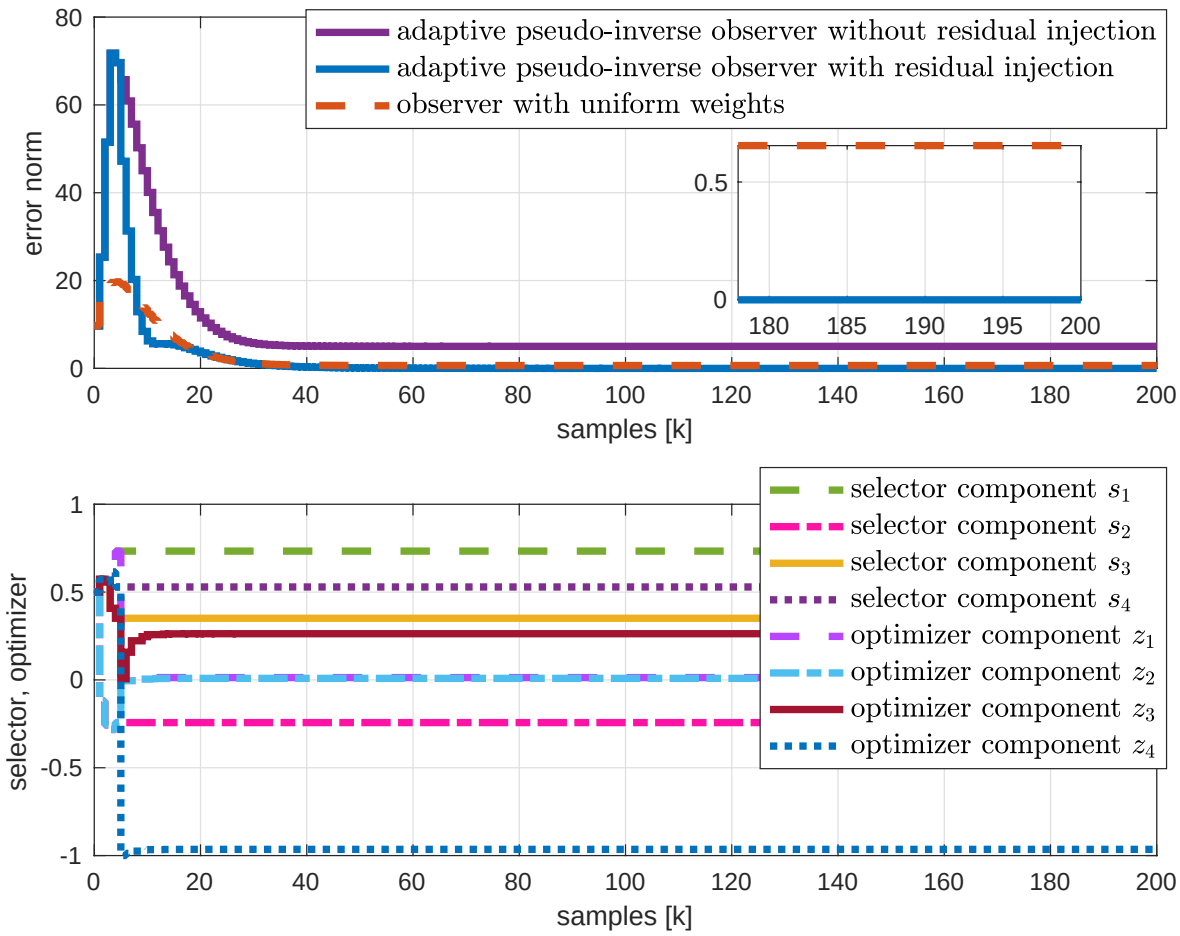

Fig. 5. Scenario 2 with constant φ: norm of estimation error (top) and selector/optimizer states (bottom)

[18] C. Commault, J. M. Dion, O. Sename, and R. Motyeian, "Observer-based fault detection and isolation for structured systems," *IEEE Trans. on Automatic Control*, vol. 47, no. 12, pp. 2074–2079, 2002.
[19] A. Pertew, J. Marquez, H, and Q. Zhao, "LMI-based sensor fault diagnosis for nonlinear lipschitz systems," *Automatica*, vol. 43, no. 8, pp. 1464–1469, 2007.
[20] E. Franco, R. Olfati-Saber, T. Parisini, and M. M. Polycarpou, "Distributed fault diagnosis using sensor networks and consensus-based filters," in *IEEE Conf. Decision and Control*, 2006, pp. 386–391.
[21] M. Demetriou, "Robust adaptive techniques for sensor fault detection and diagnosis," in *Proc. 47th IEEE Conf. on Decision and Control*, vol. 1, 1998, pp. 1143–1148.
[22] X. Zhang, "Sensor bias fault detection and isolation in a class of nonlinear uncertain systems using adaptive estimation," *IEEE Trans. on Automatic Control*, vol. 56, no. 5, pp. 1220–1226, 2011.
[23] V. Reppa, M. M. Polycarpou, and C. G. Panayiotou, "Adaptive approximation for multiple sensor fault detection and isolation of nonlinear uncertain systems," *IEEE Trans. on Neural Networks and Learning Systems*, vol. 25, no. 1, pp. 137–153, 2014.
[24] R. Luo, S. Misra, M.and Qin, R. Barton, and D. Himmelblau, "Sensor fault detection via multiscale analysis and nonparametric statistical inference," *Industrial & Engineering Chem. Res.*, vol. 37, no. 3, pp. 1024–1032, 1998.
[25] A. Cristofaro and L. Zaccarian, "An adaptive pseudo-inverse method for the fault-tolerant output allocation in linear observers with redundant sensors," *IEEE Conf. on Decision and Control*, pp. 5402–5407, 2016.
[26] ——, "Unbiased observer synthesis using dynamic output allocation for discrete-time linear plants with redundant sensors," in *2017 IEEE 56th Annual Conference on Decision and Control (CDC)*. IEEE, 2017, pp. 1743–1748.
[27] A. Alessandri and L. Zaccarian, "Stubborn state observers for linear time-invariant systems," *Automatica*, vol. 88, pp. 1–9, 2018.
[28] J. P. Hespanha, *Linear Systems Theory*. Princeton Press, 2009.
[29] M. Shakarami, K. Esfandiari, A. A. Suratgar, and H. A. Talebi, "Peaking attenuation of high-gain observers using adaptive techniques: State estimation and feedback control," *IEEE Transactions on Automatic Control*, vol. 65, no. 10, pp. 4215–4229, 2020.
[30] D. Astolfi, L. Marconi, L. Praly, and A. R. Teel, "Low-power peaking-free high-gain observers," *Automatica*, vol. 98, pp. 169–179, 2018.
[31] M. Maggiore, M. Sassano, and L. Zaccarian, "Reduction theorems for hybrid dynamical systems," *IEEE Transactions on Automatic Control*, vol. 64, no. 6, pp. 2254–2265, 2019.
[32] H. Shim, J. Seo, and A. Teel, "Nonlinear observer design via passivation of error dynamics," *Automatica*, vol. 39, no. 5, pp. 885–892, 2003.
[33] R. Goebel, R. Sanfelice, and A. Teel, *Hybrid Dynamical Systems: modeling, stability, and robustness*. Princeton University Press, 2012.
[34] R. Rockafellar and R.-B. Wets, *Variational analysis*. Springer Science & Business Media, 2009, vol. 317.
[35] A. Dontchev and R. Rockafellar, *Implicit functions and solution mappings: A view from variational analysis*. Springer, 2009, vol. 616.

Andrea Cristofaro received the M.Sc. in Mathematics from Sapienza University of Rome (Italy) in 2005 and the PhD in Information Science and Complex Systems from University of Camerino (Italy) in 2010. After some years spent in France (INRIA Grenoble) and Norway (NTNU and University of Oslo) holding different academic positions, in 2019 he joined the Department of Computer, Control and Management Engineering, Sapienza University of Rome (Italy), where he is currently an Associate Professor.

Andrea Cristofaro is author of more than 110 scientific papers, and he serves as Associate Editor for Automatica and IEEE Transactions on Control Systems Technology. He is also member of the IEEE CSS Conference Editorial Board and of the Board of Experts of the European Science Foundation. He is recipient of a Marie-Curie fellowship, and his main research interests include: fault-tolerant control, observers for linear and nonlinear systems, multi-agent and multi-robot systems, control of distributed parameter systems, hybrid systems.

Luca Zaccarian (Fellow, IEEE) received the Ph.D. degree in computer and control engineering from the University of Roma Tor Vergata (Italy) in 2000, respectively. From 2000 to 2011 he has been Assistant Professor and then Associate Professor at that same university. Since 2011 he is Directeur de Recherche at the LAAS-CNRS, Toulouse (France) and since 2013 he holds a part-time professor position at the University of Trento, Italy. Luca Zaccarian's main research interests include analysis and design of nonlinear and hybrid control systems, modeling and control of mechatronic systems. He was a recipient of the 2001 O. Hugo Schuck Best Paper Award given by the American Automatic Control Council.